Measurement Report: Extreme Heat and Wildfire Emissions Enhance Volatile Organic Compounds in a Temperate Forest

Christian Mark Salvador[1,#], Jeffrey Wood[2], Emma Cochran[2,a], Hunter Seubert[2,b], Bella Kamplain[2,c], Sami Overby[2], Kevin Birdwell[1], Lianhong Gu[1], Melanie A.Mayes[1,#]

[1]*Environmental Sciences Division, Oak Ridge National Laboratory, Oak Ridge, TN, USA*
[2]*School of Natural Resources, University of Missouri, Columbia, MO, USA*
[a]*now at: University College Dublin, Belfield, Dublin 4, Ireland*
[b]*now at: Lawrence Berkeley National Laboratory, Berkeley, CA, USA*
[c]*now at: University of Colorado Boulder, Colorado, USA*

[#]*Correspondence to:* Christian Mark Salvador (salvadorcg@ornl.gov) and Melanie A. Mayes (mayesma@ornl.gov)

Abstract. Climate extremes are projected to cause unprecedented deviations in the emission and transformation of volatile organic compounds (VOCs), which trigger feedback mechanisms that will impact the atmospheric oxidation and formation of aerosols and clouds. However, the response of VOCs to future conditions such as extreme heat and wildfire events is still uncertain. This study explored the modification of the mixing ratio and distribution of several anthropogenic and biogenic VOCs in a temperate oak–hickory–juniper forest as a response to increased temperature and transported biomass burning plumes. A chemical ionization mass spectrometer was deployed on a tower at a height of 32 m in rural central Missouri, United States, for the continuous and in situ measurement of VOCs from June to August of 2023. The maximum observed temperature in the region was 38°C, and during multiple episodes the temperature remained above 32°C for several hours. Biogenic VOCs such as isoprene and monoterpene followed closely the temperature daily profile but at varying rates, whereas anthropogenic VOCs were insensitive to elevated temperature. During the measurement period, wildfire emissions were transported to the site and substantially increased the mixing ratios of acetonitrile and benzene, which are produced from burning of biomass. An in-depth analysis of the mass spectra revealed more than 250 minor compounds, such as formamide and methylglyoxal. Extreme heat and presence of wildfire plumes modified the overall volatility, reactivity, O:C, and H:C ratios of the extended list of VOCs . The calculated OH reactivities during extreme temperature condition and transport of biomass burning plumes were 106.37 ± 4.27 s^{-1} and 106.22 ± 5.15 s^{-1}, respectively, which are substantially higher than background level of 98.78 ±1.16 s^{-1}. Multivariate analysis also clustered the compounds into five factors, which highlighted the sources of the unaccounted-for VOCs. Ultimately, results here underscore the effect of extreme heat and wildfire emissions on the overall chemical properties VOC in a temperate forest.

1. Introduction

Future global climate, with continuing greenhouse gas emissions such as CO_2 from the burning of fossil fuels, is expected to have warmer temperatures that impact critical atmospheric processes. Global averaged surface air temperature is projected to exceed 1.5°C relative to 1850–1900 by the year 2030, regardless of the emission scenarios. Looking further to the future, 2081 to 2100 will experience an additional increase of 0.2°C–1.0°C and 2.4°C–4.8°C in low and high emissions scenarios, respectively (Lee et al., 2021). The heating of the atmosphere in the future will have severe effects on several atmospheric constituents and processes. For instance, a series of models have shown that warming due to greenhouse gas emissions will induce an increase in the global annual average mixing ratios of particles with less than 2.5 μm diameter ($PM_{2.5}$) (Park et al., 2020), which will have implications for air quality, climate, and human cardiovascular health. By 2050, the elevated temperature is projected to increase $PM_{2.5}$ by 2–3 μg m^{-3} in the summer of the eastern United States as a consequence of faster oxidation rates and elevated production of organic aerosols (Shen et al., 2017). There is thus an urgent need to elucidate the impact of extreme heat on atmospheric processes, including the emission and transformation of organic compounds, to understand future aerosol-generating scenarios.

One potential effect of overall atmospheric warming is the change in global wildfire frequency (Varga et al., 2022; Sarris et al., 2014; Ruffault embus al., 2018). At elevated temperatures, evaporation of soil moisture and generation of more fuel from drying vegetation are more pronounced, thus inducing more wildfire events (Juang et al., 2022). Beyond the CO_2 emissions, wildfires generate thousands of carbonaceous compounds that impact global climate air quality and human health (Schneider et al., 2024a). With the elevated prevalence of wildfires with prolonged duration, extreme wildfire events are expected to impact the future mixing ratio and distribution of atmospheric chemical compounds that influence relevant processes such as aerosol and cloud formation. For instance, global-scale airborne measurements showed increased tropospheric ozone in air masses influenced by biomass-burning (BB) events (Bourgeois et al., 2021). Long-term analysis of wildfire events in Western Canada (2001–2019) also indicated an increase in the average ozone mixing ratio (~2 ppb), particularly during events with high mixing ratios of atmospheric aerosols from wildfire (Schneider et al., 2024b). Ozone enhancement may lead to elevated atmospheric oxidation capacity that can initiate more secondary pollutant formation.

Among the chemical components of the atmosphere, the abundance of volatile organic compounds (VOCs) is expected to respond to extreme heat and wildfire emissions. VOCs, particularly the unsaturated compounds, interact with oxidants such as hydroxyl (OH) and nitrate (NO_3) radicals, which subsequently create ozone and oxidized molecules (Hakola et al., 2012; Ramasamy et al., 2016; Spirig et al., 2004; Vermeuel et al., 2023). Further reaction products such as highly oxidized molecules also participate in the formation of particles that subsequently act as cloud condensation nuclei (Chen et al., 2022; Hallquist et al., 2009). The emission and transformation of VOCs highly depend on environmental parameters such as temperature, relative humidity, and solar radiation. For instance, biogenic volatile organic compounds (BVOCs) exhibit an exponential temperature dependence, whereby an increase in temperature accelerates both their production and release from plant tissues. (Guenther et al., 1993; Rinnan et al.,

2020). However, the degree of changes under future climate conditions is still uncertain (i.e., suppression or enhancement) (Daussy and Staudt, 2020). A global estimate of isoprene emissions with temperature and land-cover drivers under future scenario (year: 2070-2099) was 889 Tg yr^{-1}, substantially higher compared to that expected using current climatological and land-cover conditions (522 Tg yr^{-1}) (Wiedinmyer et al., 2006). Moreover, CO_2, which is expected to rise in the future climate, can substantially decrease the emission of isoprene from vegetation (Lantz et al., 2019a). On the other hand, empirical results and modeling efforts suggest that future elevated temperatures could suppress the impact of CO_2 on isoprene emissions, thus increasing the uncertainty of future climate's influence on the emission of isoprene (Lantz et al., 2019b; Sahu et al., 2023). Moreover, BB events such as wildfires are considered as the second-largest source of VOCs globally, further influencing air quality and climate (Jin et al., 2023; Yokelson et al., 2008). During wildfire events, the burning of vegetation and other biomass induce the pyrolysis of plant materials which ultimately release hundreds of VOCs during the process (Ciccioli et al., 2014) (Hatch et al., 2015; Koss et al., 2018; Selimovic et al., 2018; Binte Shahid et al., 2024). Typical VOCs emitted from wildfires include acrolein, acetonitrile, pyrrole, styrene, guaiacol, toluene, phenol, and catechol (Liang et al., 2022; Jin et al., 2023). Benzene, a common compound emitted during wildfire events, has been found to be more than ten times the typical concentration in metropolitan areas, thereby posing elevated health risks (Ketcherside et al., 2024). Beyond their health impacts, the emitted reactive carbon- and nitrogen-containing compounds can significantly alter several critical atmospheric processes, including ozone formation and particle formation events. However, the relative importance and contribution of volatile organic compounds (VOCs) from wildfire activities to atmospheric reactivity remain uncertain, even with several studies tackling the problem. (Gilman et al., 2015; Kumar et al., 2018; Permar et al., 2023) . A comprehensive understanding of the interactions between future abiotic factors and VOC emissions is essential for accurately predicting future air quality and climate scenarios.

In this work, we conducted a field campaign in the summer of 2023 to quantify the variability of VOCs over a temperate oak–hickory–juniper (*Quercus–Carya–Juniperus*) forest in the Ozark Border Region of central Missouri. The primary goal of the campaign was to examine the influence of temperature on VOCs. We deployed a high-resolution chemical ionization mass spectrometer to continuously measure VOC concentrations. We were also able to incorporate opportunistic analyses of the impact of wildfire emissions on the variability of VOCs due to the smoke that reached our site because of extreme forest biomass burning activity in Canada.

2. Experimental Designs

2.1 Site Description and Meteorological Data

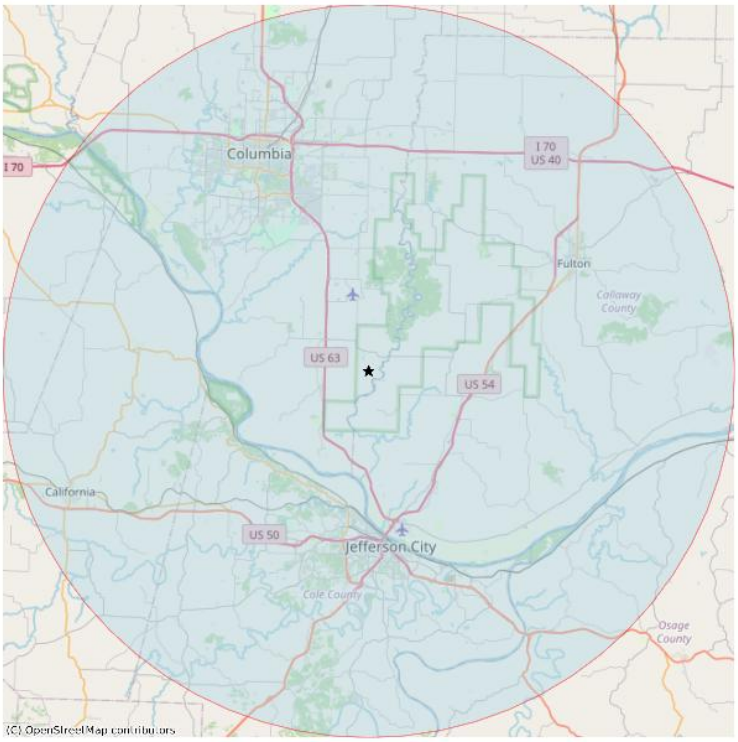

Figure 1. *Map of the MOFLUX site located in Missouri. The circle indicates a 50 km radius from the site. The figure illustrates the interstate and forested areas, which may contribute to the sources of anthropogenic and biogenic VOCs in the temperate forest.*

Measurements were conducted at the Missouri Ozark AmeriFlux (MOFLUX) site (latitude: 38° 44' 38.76" N, longitude: 92° 12' 0" W) in central Missouri, United States (see Figure 1). The MOFLUX site is registered with the AmeriFlux (ID: US-MOz) and PhenoCam networks (ID: missouriozarks). The campaign was conducted during the summer of 2023, between June 25 and August 12. The site is situated in the Baskett Wildfire Research and Education Area. The primary sources of BVOCs were oaks (white and black), sugar maple, shagbark hickory, and eastern red cedar (Geron et al., 2016). The subtropical/mid-latitude continental characteristics of the area provide a warm and humid overall climate for the forest. Long-term measurements of meteorological parameters (1981–2010) at a nearby airport (~10 km) indicated that the average temperature for July was 25.2°C (National Climatic Data Center citation). Typical precipitation (annual average: 108.2 cm) is fairly evenly distributed through the yearly cycle. More information regarding the site is provided elsewhere (Gu et al., 2015).

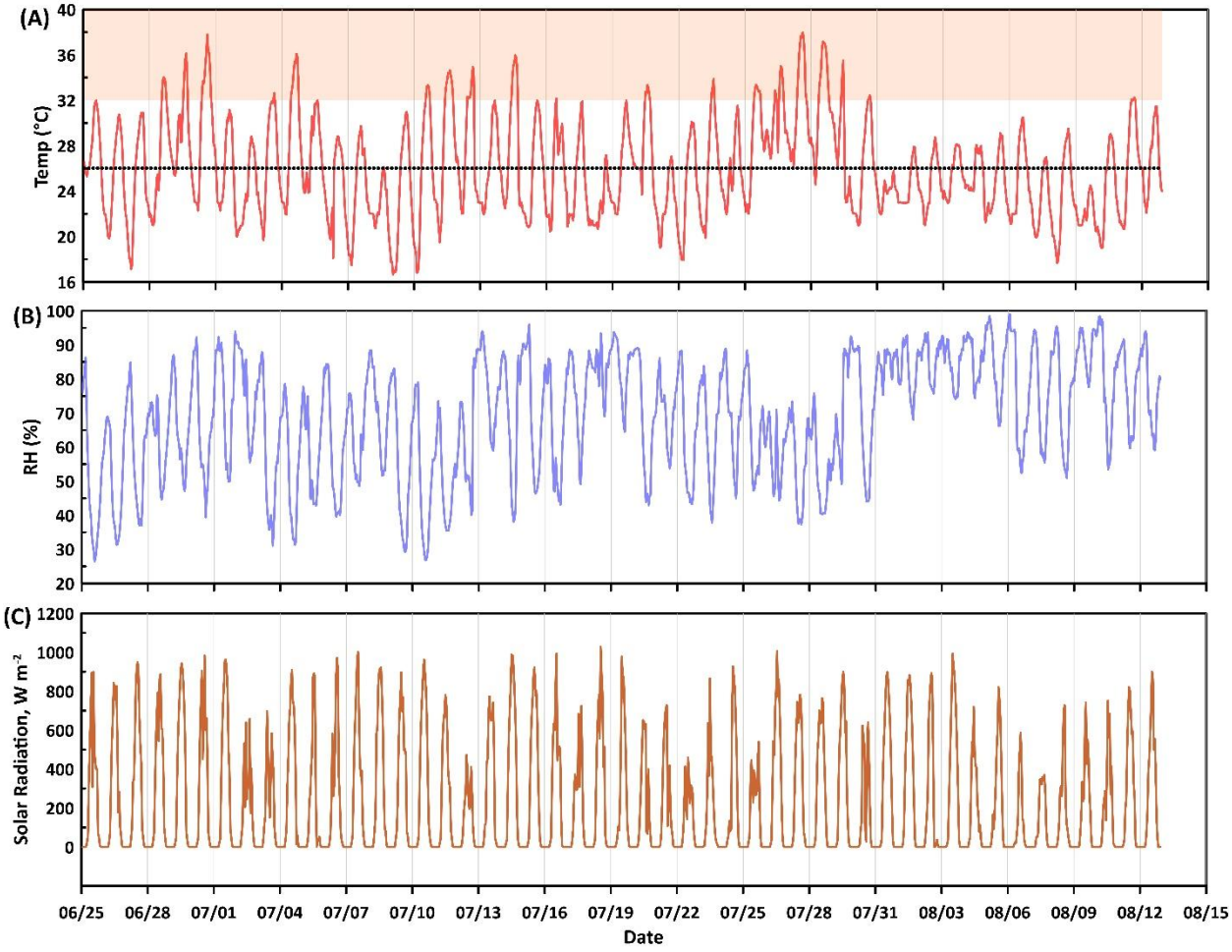

Figure 2. *Time series profile of (A) temperature, (B) relative humidity, RH, and (C) downward solar radiation at the temperate mixed deciduous forest in Missouri. The dotted line in the temperature plot is the average value during the measurement duration, and the shaded filled area denotes the extreme temperature conditions (>32°C).*

The Ozark Plateau (Wiedinmyer et al., 2005), and this site in particular, is a known hotspot for emissions of BVOCs such as isoprene and monoterpene. Drought is a critical event at MOFLUX, as such environmental stress induced the highest ecosystem isoprene emission ever recorded for a temperate forest in 2011 (53.3 mg m^{-2} h^{-1}) (Potosnak et al., 2014). Field measurement campaign in 2012 in MOFLUX reported isoprene reaching a maximum concentration of 28.9 ppbv, while monoterpenes peaked at 1.37 ppbv over half-hour intervals (Seco et al., 2015). Moreover, the site is about 5 km away from a major highway, thus anthropogenic VOCs (AVOCs) such as benzene and toluene from vehicle exhausts are expected to be transported into the forest. Given these strong emitters of BVOCs and the evident transport of AVOCs into the forest, the study area proved to be a good test bed for measurement of the overall response of VOCs to abiotic stress in a way that simulates possible future atmospheric conditions.

Figure 2 shows the time series profile of hourly averages of temperature and relative humidity collected from Columbia Regional Airport (latitude: 38° 49' 1.2" N, longitude: 92° 13' 15.6" W) approximately 8.5 km from the MOFLUX site. Downward solar radiation data were measured at a weather site in Ashland, MO (latitude: 38° 43'

19.2" N, longitude: 92° 15' 10.8" W), 5.22 km from the MOFLUX tower The data were accessed using the MesoWest online website (https://mesowest.utah.edu/) provided by the Department of Atmospheric Sciences, University of Utah. The average (absolute min-max) temperature, relative humidity (RH), downward solar radiation, and wind speed (not shown in the figure), were 26°C (16–38°C), 69.01% (26.43–99.02), 228 W m^{-2} (0–1028 W m^{-2}), and 3.2 m s^{-2} (0–11.27 m s^{-2}) during the time of VOC measurements. The diurnal profiles of the meteorological conditions are provided in the supplement. During the weeks of July 4 and July 11, 64 and 100% cumulative percent area reported abnormally dry conditions (D0, US Drought Monitor Category). Drought data were accessed from the U.S. Drought Monitor (https://droughtmonitor.unl.edu/). Smoke concentrations (in mg m^{-3}) were estimated from the High-Resolution Rapid Refresh (HRRR) 3-km weather model for Missouri at 6-hour intervals for the duration of the VOC data measurement period The HRRR model generates weather forecast for the entire continental US. The Smoke model is based on single smoke tracer, plume rise parametrization, and satellite fire radiative power processing (Chow et al., 2022). Values ranged from 0 to 10 mg m^{-3} during 80% of the measurement dates (overall average was 7.33 mg m^{-3}) but reached a maximum of 175 mg m^{-3} on July 16 in association with drift from large Canadian wildfires. Backward airmass trajectories were estimated using the Hybrid Single-Particle Lagrangian Integrated Trajectory (HYSPLIT) model (Stein et al., 2015). The backward trajectories were calculated based on single trajectory, 500 m above ground level height, 24-hour duration and model vertical velocity as the motion calculation method. The meteorology used for the calculation was based on 1-degree Global Data Assimilation System (GDAS1).

2.2 VOC Measurement and Identification

VOCs were measured using a proton transfer reaction time of flight mass spectrometer (PTR-ToF-MS 6000 X2) (Ionicon Analytik Ges.m.b.H., Innsbruck, Austria). The mass resolution of the technique (6000 m/Δm) provided an extended list of VOCs, beyond the usual routinely evaluated compounds (e.g., methanol, isoprene, and monoterpene).The PTR-ToF-MS was located in a climate-controlled cabin at the base of the MOFLUX tower. A detailed description of the general mechanism of the PTR-ToF-MS can be found in the supplementary file and elsewhere (Yuan et al., 2017). The PTR-ToF-MS was calibrated regularly every two weeks for 50 minutes using a 110-ppb mixture of gases (isoprene, limonene, benzene, toluene, ethylbenzene, dichlorobenzene, trichlorobenzene, and trimethylbenzene, Restek Corp). The linear calibration curve for each standard compound consisted of eleven data points, with mixing ratios ranging between 1.89 and 50.9 ppb. The same compounds were used to calculate the mixing ratio of other compounds using the transmission efficiency and first-order kinetic reaction. PTR-ToF-MS can provide quantitative measurement of compounds without standard gas available using mass dependent transmission analysis. Instrument blank was measured hourly using a series of switching valves and Ultra Zero grade air (Airgas).

Ambient air was sampled from the MOFLUX tower with the height of 32 meters. The air was drawn at the top of the tower using a 65-meter overall length with ½ in. OD PFA tube (McMaster-Carr) and a GAST compressor/vacuum pump with a mass flow controller (Alicat Scientific, Inc) set at 20 L min^{-1}. A Teflon filter with 47 mm diameter was

attached to inlet to prevent particles from entering the sampling line. The VOC data was collected using 100 millisecond time resolution and averaged hourly during the data processing and reporting.

High-resolution peak analysis, chemical formula identification, and data quantification were performed using the IONICON data Analyzer (IDA). IDA identified more than 1000 ions, which were subsequently reduced to 275 peaks with more than 5 parts per trillion (ppt) mixing ratios above the average blank data

The chemical identification procedure was complemented by an analysis using ChemCalc, which also provided the theoretical masses and degree of saturation (Patiny and Borel, 2013).

The volatility of the extended list of VOCs was assessed by estimating the effective saturation mass mixing ratio (C_{sat}). The parameterization of the volatility, based on the number of carbon, oxygen, and nitrogen atoms (Donahue et al., 2011; Mohr et al., 2019), was calculated using the following equation:

$$log(C_{sat}) = (n_{O*} - n_C)b_C - (n_O - 3n_N)b_O - 2\frac{(n_O - 3n_N)n_C}{(n_C + n_O - 3n_N)}b_{CO} - n_N b_N \qquad (3)$$

where $n_{0*} = 25$, $b_C = 0.475$, $b_O = 0.2$, $b_{CO} = 0.9$, and $b_N = 2.5$. The terms n_C, n_O, and n_N are the number of carbon, oxygen, and nitrogen atoms, respectively.

The total calculated OH reactivity (R) was obtained from the measured concentration of the VOCs using the following equation similar to a prior study (Wang et al., 2021):

$$R = \Sigma k_{VOC_i+OH}[VOC_i] \qquad (4)$$

where $[VOC_i]$ is the concentration of the volatile organic compounds measured by the PTR-ToF-MS and k_{VOC+OH} (cm^3 $molecule^{-1}$ s^{-1}) are the reaction rate constant between the OH and VOC. The reaction rate constant were calculated bases on the available data from the National Institute of Standards and Technology (NIST) Chemical Kinetics Database which compiled kinetics data on gas phase reactions (https://kinetics.nist.gov/kinetics/). All molecular formulas identified from more than 250 ions were subjected to Reaction Database Quick Search Form. The calculation of the reaction rate constant incorporated the hourly temperature conditions observed during the field campaign. Only records with available activation energy (Ea) and pre-exponential factor (A), along with temperature range (20-36 °C) similar to the observed conditions in the temperate forest, were considered in the calculation. To address molecular formulas with multiple records, the median value of the rate constants was employed. For example, the reaction rate constant for the class of monoterpene was derived from literature values of several compounds, including α-pinene, β-pinene, 3-carene, limonene, camphene, and β-ocimene. The median reaction rate constant across all these monoterpenes was then utilized to calculate the OH reactivity.

2.3 Source and Process Signature Analysis of VOCs using Multivariate Analysis

Determination of the source signature or emission profile of the VOCs is critical in assessing the dominant anthropogenic and biogenic activities that impact the atmospheric reactivity from VOCs. Here, multivariate analysis was applied to the observed VOC mixing ratios using non-negative matrix factorization (NNMF). Because NNMF

requires no uncertainty for the calculation procedure, it has an advantage over positive matrix factorization, which is typically implemented for a mixture of organic compounds in the gas and particle phase (Salvador et al., 2022). NNMF is expressed as:

$$A_{m\times n} = W_{m\times k}H_{k\times n} + \sigma_{m\times n} \quad (5)$$

where A is the input matrix with dimensions of m and n containing non-negative elements, W and H are species fingerprint and coefficient matrices, k is the lowest rank approximation or the optimal factor, and σ is the residual between the left and right sides of the equation. The VOC mixing ratio data with a matrix of 196 × 274 dimensions was employed as the input for the NNMF routine program in MATLAB. The NNMF was applied for a 10-factor series with 30 replicates, 1000 iterations, and a multiplicative update algorithm. *Replicates* are the number of times program will perform the factorization, with every replicate starting with random values for W and H. *Iteration* is the input value for the maximum iteration in the optimization settings for convergence purposes. The NNMF at MATLAB can be performed either as alternating least square (als) or multiplicative update algorithm (mult). This study implemented the *mult* factorization algorithm as it has faster iterations and more sensitive to starting values.

3. Results and Discussion

3.1 General Overview of the Major VOCs

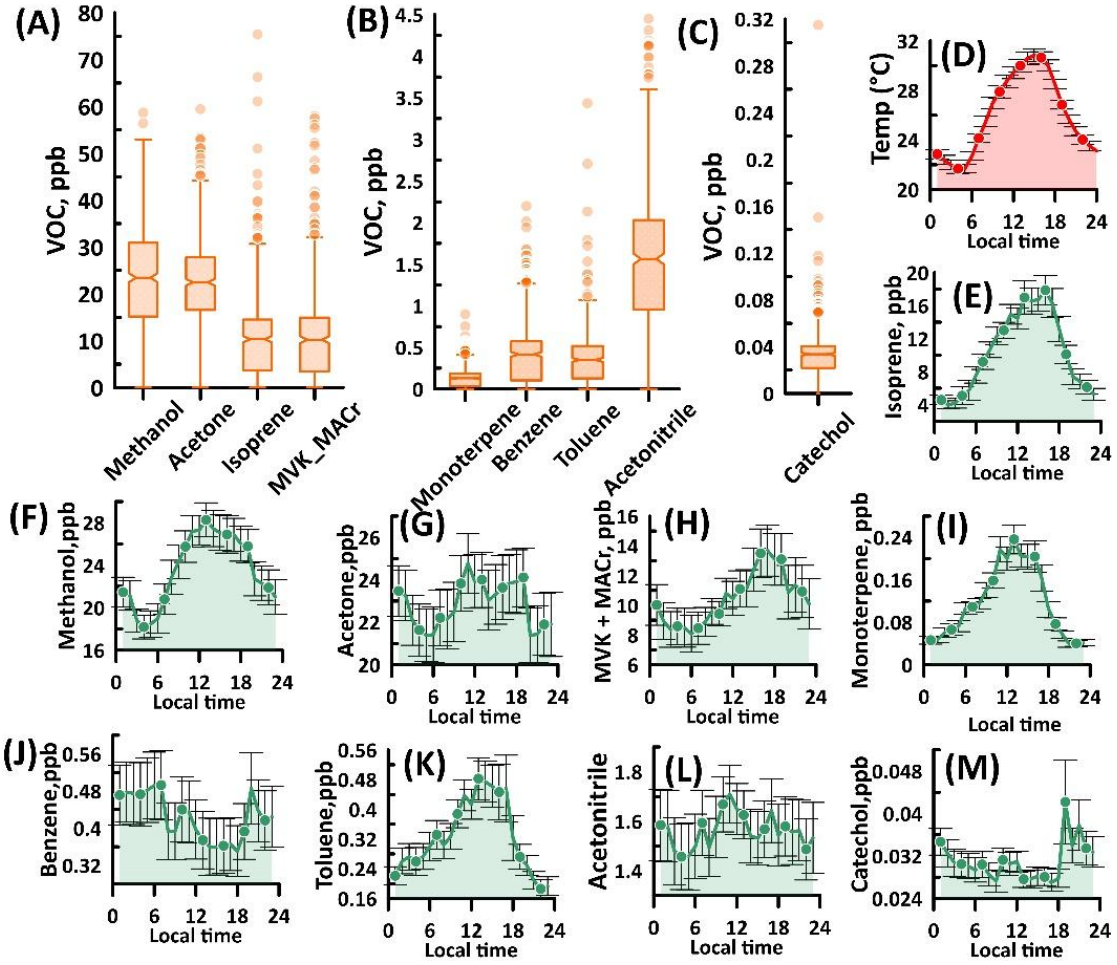

Figure 3. *(A-C) Average mixing ratio in ppb and (E-M) average diurnal profile of major VOCs at MOFLUX . Also included here is the average diurnal profile of (D) temperature for reference. Time reported here is the local daylight time. The center lines of the box and whisker plots are the mean mixing ratio. Box edges are quartiles, and lower (upper) corresponds to 25th (75th). Whiskers represent 1.5 times the interquartile range. Symbols outside the box plot are outliers. Diurnal profiles have a unit of ppb mixing ratio. MVK and MACr are methyl vinyl ketone and methacrolein. The error bars are represented by standard error.*

Many VOCs (n = 275) were detected in the ambient air throughout the three-month measurement period. Figure 3 shows the average mixing ratio of the dominant VOCs observed in the temperate forest. Among the VOCs, methanol and acetone recorded the highest mixing ratios. Methanol and acetone are the most abundant nonmethane organic gases in the troposphere and are emitted by terrestrial plants during growth stages (Bates et al., 2021; Hu et al., 2013; Wells et al., 2014). Mean mixing ratios of methanol and acetone were 23 ppb, consistent with a prior study done in MOFLUX, in which half-hour averages of methanol ranged between 1.9 and 26 ppb (Seco et al., 2015). Here, the maximum hourly average mixing ratio of methanol reached as high as 59 ppb, which occurred at 6:00 pm on the 30th of June. Methanol also showed a diurnal profile with a daily peak at noon, which was an indication of a photochemical

source. Besides the terrestrial emissions of methanol, the secondary production of methanol from organic peroxyradicals (e.g., CH_3O_2) contributes substantially to the methanol budget (Bates et al., 2021).

Also shown in Figure 3 are the average mixing ratios of isoprene and its primary oxidation products, methyl vinyl ketone and methacrolein (MVK+MACr). Isoprene is the most dominant BVOC, contributing around 50% to the total global emission (Guenther et al., 2012). Isoprene substantially influences the surface ozone concentration and secondary organic aerosol formation, which is attributed to isoprene's reactivity to ozone, OH, and nitrate (NO_3) radicals (Wennberg et al., 2018). Besides the photochemical oxidation of isoprene, MVK and MACr have other sources, such as Biomass Burning (BB) and gasoline vehicular emissions (Ling et al., 2019). Isoprene also generates MVK during nighttime through the dominant β-RO_2 isomer formation pathway (Ng et al., 2017). Isoprene's emission rate at MOFLUX was previously reported as one of the highest for canopy-scale emissions (53.3 mg m^{-2} h^{-1}) (Potosnak et al., 2014). This was evident in our measurement, where the average mixing ratio of isoprene during the intensive observation period was 10.32 ppb, and MVK + MACr had a similar mean mixing ratio. The isoprene mixing ratio reached as much as 75 ppb, which occurred at 1:00 pm on July 4. Observed isoprene mixing ratios were substantially elevated compared to other similar temperate forests in the United Kingdom (~8 ppb) (Ferracci et al., 2020), deciduous forest in Michigan, USA (~1.5 ppb) (Kanawade et al., 2011), and mixed temperate forest in Canada (~0.01 ppb) (Fuentes and Wang, 1999). For MVK+MACr, prior measurements in similar environments reported mixing ratios below 2.0 ppb (Safronov et al., 2019; Shtabkin et al., 2019; Montzka et al., 1995) highlighting the intense production of MVK+MACr at MOFLUX. Interestingly, the most elevated mixing ratio of MVK+MACr (58 ppb) occurred on a different day (6/28) and later in the night (8:00 pm); this result was attributed to other sources of MVK and MACr. Nevertheless, the MVK showed a similar diurnal profile with isoprene, which suggested that photochemical oxidation of isoprene was the dominant source of MVK+MACr observed in MOFLUX. Also, diurnal profiles, as indicated in Figure 3, showed that MVK+MACr still persisted even with the reduction of the isoprene at nighttime. This was attributed to the longer atmospheric lifetime and lesser reactivity of MVK+MACr. Furthermore, The ratio between isoprene and MACR + MVK indicates the lifetime of the isoprene and degree of oxidation of isoprene to MVK and MACr. Greater than value of 1.0 observed in MOFLUX suggests transport time shorter than one isoprene lifetime, as indicated in the previous studies (Selimovic et al., 2022; Hu et al., 2015).

Monoterpene, a critical contributor to ozone and secondary aerosol formation (Salvador et al., 2020a; Salvador et al., 2020b), is a class of organic compounds with the formula $C_{10}H_{16}$ such as α-pinene, β-pinene, limonene, δ-carene, ocimene, and sabinene, and its distribution varies significantly based on the vegetation species. At MOFLUX, monoterpene had an average mixing ratio of less than 0.2 ppb, as shown in Figure 3. Throughout the measurement duration, the maximum mixing ratio of monoterpene was 0.9 ppb. This ambient level is similar to a prior measurement at the MOFLUX site (Seco et al., 2015), as well as observations of monoterpene in other temperate forests in Wisconsin, USA, and Wakayama, Japan (Vermeuel et al., 2023; Ramasamy et al., 2016). Particle size distribution analysis (see Figure S2) at our temperate forest indicated no evident particle formation events. Particles >50 nm in diameter were observed with no apparent aerosol growth (see Figure S2). The average geometric mean diameter in

MOFLUX site was 85.53 ± 16.68 nm. Prior study also showed less frequent new particle formation events, particularly during the influence of southerly air masses rich in BVOCs (Yu et al., 2014). The most probable reason for the presence of these particles was the isoprene-rich condition of the temperate forest that impacted the aerosol nucleation, even with enough monoterpene and ozone available for particle formation. Prior plant chamber analysis indicated that the suppression of new particle formation was dependent on the ratio of isoprene carbon to monoterpene carbon (Kiendler-Scharr et al., 2009). The mixing of isoprene and monoterpene also impacts the atmospheric oxidation capacity, in which isoprene scavenges the OH radicals (Mcfiggans et al., 2019). Recent studies also showed that the mixing of isoprene to monoterpene reduced C_{20} dimers that drive aerosol formation at mixed biogenic precursor systems (Heinritzi et al., 2020). At MOFLUX, the median ratio of isoprene carbon to monoterpene carbon was 42, which is significantly higher compared to measurements in forests in Alabama (Lee et al., 2016), Michigan (Kanawade et al., 2011), the Amazon (Greenberg et al., 2004), and Finland (Spirig et al., 2004). Ratios above 20 completely limit the formation of aerosols, which is consistent with the observations at MOFLUX.

Besides biogenic VOCs, several anthropogenic-related VOCs were detected in the temperate forest. The site is about 5 km away from a major highway, which possibly contributed to the diversity of VOCs at MOFLUX. During the measurement period, benzene, a VOC usually emitted from automobile exhausts, had a mean mixing ratio of 0.42 ppb, with a maximum of 2.2 ppb. Benzene had mixing ratio peaks consistent with the traffic (8:00 and 20:00) with no evident noontime peak. Similar to biogenic precursors, benzene can also initiate particle formation events, particularly at low NOx conditions (Ng et al., 2007; Li et al., 2016). The mixing of the biogenic (e.g., isoprene and monoterpene) and anthropogenic VOCs (e.g., benzene) at MOFLUX can introduce unaccounted-for molecular interactions (Voliotis et al., 2021) that can influence the formation of aerosols in the forest. Toluene, another important aromatic VOC from urban emissions, was also observed at a significant amount at the site (~0.3 ppb, mean) with a max mixing ratio of 3.4 ppb. The noontime peak of the toluene daily cycle was unexpected because it usually tracks with traffic conditions. Interference of para-cymene fragmentation in the drift tube of the PTR-ToF-MS at mass 93 (Ambrose et al., 2010) might have impacted the observed concentrations at MOFLUX although we also do not discount the emission of toluene from vegetation (Heiden et al., 1999) .

3.2 Impact of Extreme Temperatures on VOCs

During some parts of the measurement period, mid-Missouri experienced extreme temperature conditions that impacted the physiochemical processes of the vegetation and the atmosphere. During the measurement period, the average temperature was 26°C, and the highest hourly value was 38°C. The average temperature was close to the reported long-term mean temperature in the region; however, the period of measurement exhibited extreme temperatures that impacted VOC emissions. Diurnal profile temperature showed a daily peak occurring at 15:00, which typically had a 29.9°C mean temperature. The extreme temperature, defined by an hourly mean temperature over 32 °C, was similar to the projected climate scenarios that temperature will increase by 2–4°C by 2100 (Collins et al., 2013). The extreme temperature defined in this study aligns with the heatwave definition (Perkins and Alexander, 2013; Perkins-Kirkpatrick and Gibson, 2017), wherein the 90th percentile temperature for the month of

July from 2015 to 2024 is 32°C. The extreme temperature occurred for more than 100 hours (see Figure S1 for histogram).

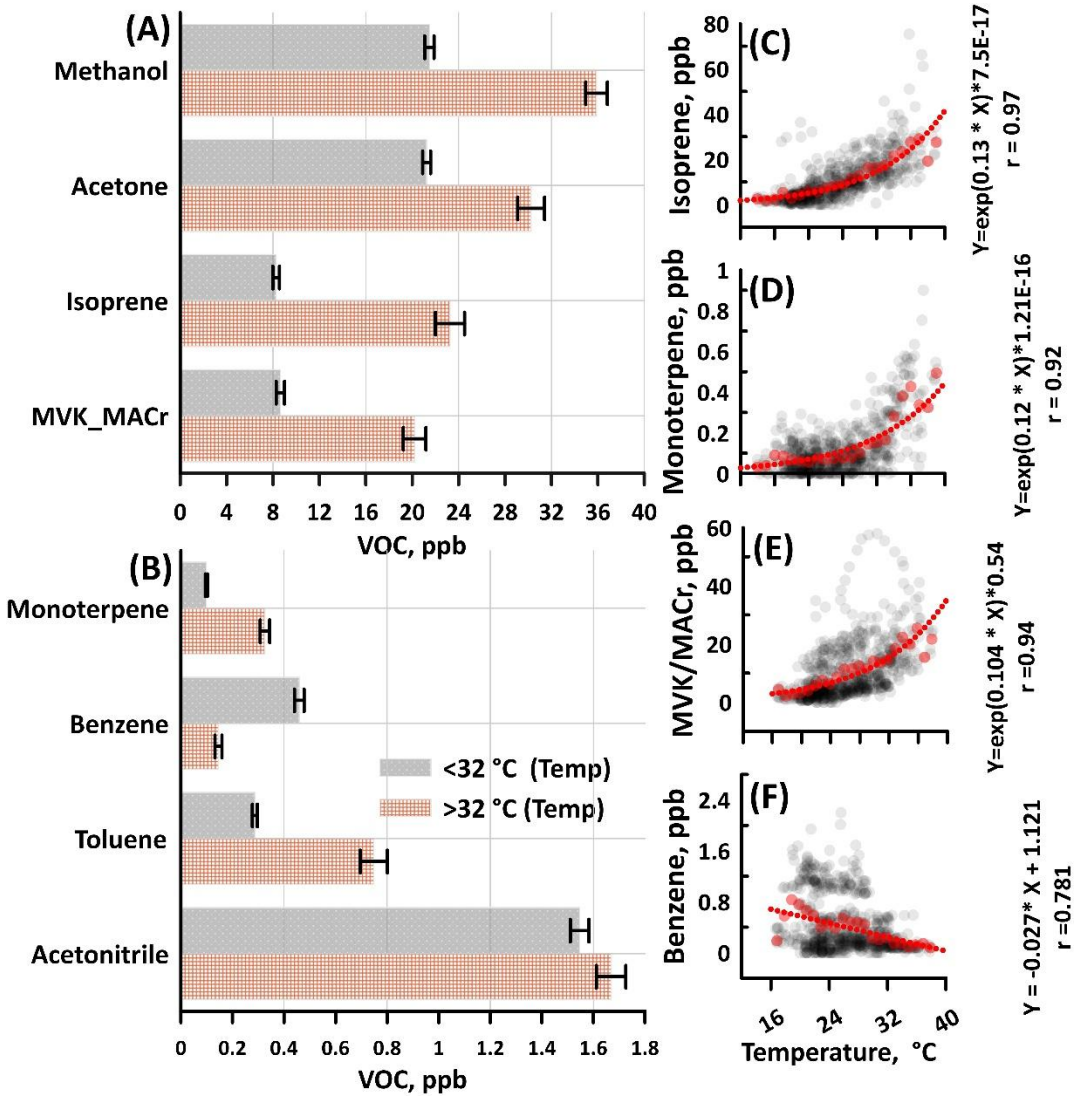

Figure 4. *(A-B) Comparison of VOC mixing ratios for temperatures below and above 32°C. Catechol, not shown here, showed no evident difference between the two conditions (~30 ppt). The error bars in the bar chart are represented by standard error. (C-F) The correlation analysis of temperature with biogenic VOCs and benzene mixing ratios (in ppb). Correlation analysis of other major VOCs is provided in the supplement. Black symbols are the hourly data, whereas the red lines indicate the best-fit line of the binned mixing ratio of VOCs according to 1.0°C of temperature. The equation of the exponential fit line and correlation coefficients are given on the right side of the plot.*

The major BVOCs, isoprene and monoterpene, increased with temperature, as shown in Figure 4. Under extreme temperatures, the isoprene and monoterpene mixing ratios were 23 and 0.32 ppb, respectively, which were three times higher than the concentrations observed at temperatures below 32°C. The enhancement of isoprene and monoterpene also increased the reactivity of the atmosphere in the temperate forest, based on the calculated 8.31 s^{-1} increase in OH reactivity. Furthermore, Figure 4 shows the evident exponential relationship between temperature and the major BVOCs, consistent with previous studies in which temperature controls the emission of isoprene and monoterpene

(Hu et al., 2015; Selimovic et al., 2022; Guenther et al., 2012). The empirically determined coefficients (β) for isoprene and monoterpene are 0.13 and 0.12, respectively. The emission of isoprene is linked to plant thermotolerance, which is the ability of plants to endure and adapt to high temperatures without experiencing detrimental effects on their growth (Sharkey et al., 2007; Duncan et al., 2009). While the dependence of monoterpene emissions on temperature appears similar, based on the empirically determined coefficients calculated in this study, the mechanisms for monoterpene release from vegetation differ from those of isoprene. This variation is primarily due to plants' ability to store monoterpenes and their high- water solubility and elevated temperature leads to vaporization of stored monoterpenes. (Loreto and Schnitzler, 2010; Malik et al., 2019; Malik et al., 2023)

MVK and MACr produced from the oxidation of isoprene showed a strong association with temperature. MVK and MACr reached a 20-ppb average mixing ratio during extreme temperature conditions. As shown in Figure 4, the concentration of MVK/MACr doubled during extreme temperature conditions compared at low temperatures. This is consistent with a prior study that showed the yield of MVK increased with temperature (Navarro et al., 2013) .

Anthropogenic tracers such as benzene and xylene did not show dependence on temperature, unlike some BVOCs. Remarkably, the toluene mixing ratio (0.73 ppb) doubled at higher temperatures, unlike the benzene and xylene. This result further supports our initial claim that the compound occurring at mass 93 originates from the fragmentation of monoterpene or from the emission of toluene from biogenic activities. The correlation plot in the supplement (Figure S4) shows a direct relationship between the two compounds.

Overall, extreme temperature conditions had a mixed impact on the VOCs observed in the temperate forest. Urban and wildfire markers showed insensitivity to temperature variation. On the other hand, BVOCs such as isoprene, MVK+MACr, and monoterpene showed exponential responses but at varying rates. The alteration of VOC distribution due to enhanced temperature has implications on the formation of secondary aerosols, particularly under expected elevated temperatures under future climate regimes. Recent laboratory chamber studies have shown that unexpected interaction of individual VOCs (e.g., isoprene, monoterpene, toluene, xylene, and trimethylbenzene) during the oxidation process produced intermediates and products that impacted the yields, volatility, and other physiochemical properties of aerosols (Voliotis et al., 2021; Takeuchi et al., 2022; Chen et al., 2022).

3.3 Transport of Emissions from Forest Fires

In 2023, severe wildfires that were initiated by summer lightning storms occurred over several boreal forests in Canada, which resulted in burning of more than 156,000 km^2 of cumulative area that accounted for at least 1.7% of Canada's land area (Wang et al., 2023). Between May and September of 2023, carbon emissions from fires reached more than 638 Tg C based on satellite observations (Byrne et al., 2023). In MOFLUX, typical gas phase BB tracers were observed in substantial amounts. Acetonitrile, one of the prominent BB markers (Huangfu et al., 2021), had mean and maximum mixing ratios of 1.56 ppb and 4.45 ppb, respectively. Such values are beyond the mixing ratio range (0.047 to 1.08 ppb) of acetonitrile recorded in Asian, US, and European regions (Huangfu et al., 2021), implying the severe impact of BB. Acetonitrile did not exhibit a typical daily cycle, aligning with the unpredictable emissions

and transport dynamics characteristic of biomass burning events. Another prominent BB marker measured at the site was catechol, an aromatic compound directly emitted from wildfire processes. At MOFLUX, catechol had a mean level of 30 ppt but increased significantly to 300 ppt on some days. Catechol had a minor peak during the daytime, which can be attributed to the photochemical processing of phenol (Finewax et al., 2018), another aromatic VOC emitted during BB events. Moreover, acetonitrile (r = 0.53) and catechol (r = 0.017) also did not follow the trend of temperature

Two air pollution episodes (June 24 to July 1 and July 15 to 17) resulting from these wildfires affected the field measurement at MOFLUX. Figure 5 shows the HRRRR- derived smoke concentration measured at MOFLUX. The two pollution episodes had different levels of smoke, the second period having stronger enhancements compared to the first. Wildfire emissions during the first episode were substantially transported to Europe, whereas the second impacted the USA to a considerable extent (Wang et al., 2023). A wildfire that occurred between July 12 and 19 primarily near Fort Nelson, Northwest Canada, was transported to the MOFLUX site. Back trajectory analysis (see Figure 5) indicated that the plumes arriving at the site during the same period originated from the northwest, suggesting a significant long-range transport of wildfire products to the MOFLUX temperate forest. Atmospheric dispersion of the smoke in Missouri is presented in Figure S5.

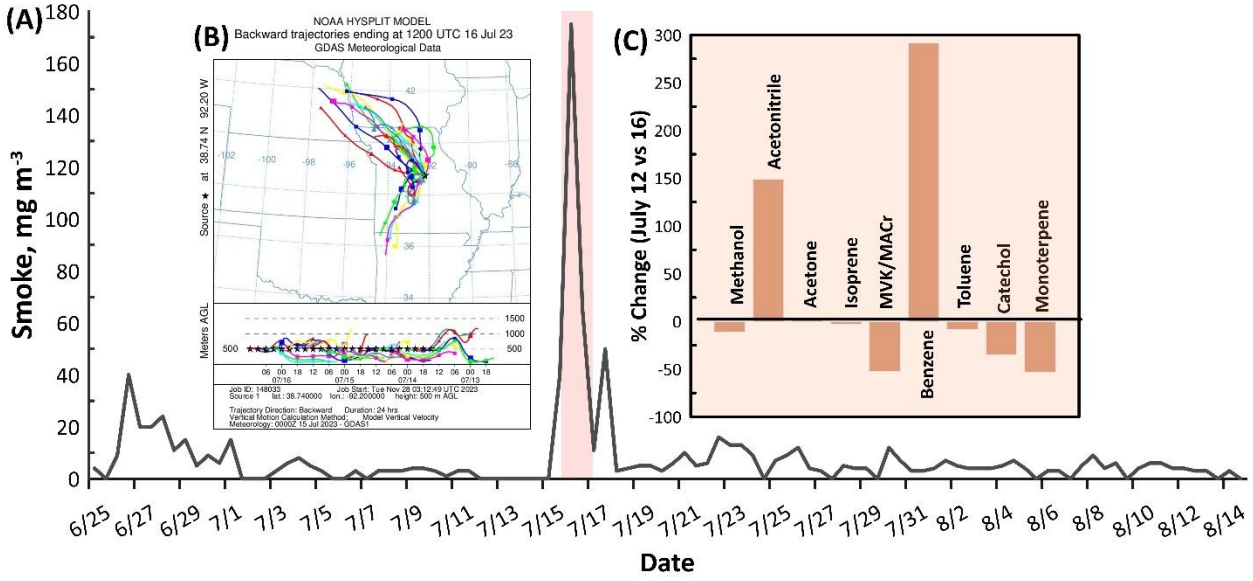

Figure 5. *(A) Smoke profile observed during the field measurement. The red highlighted area is the period with intense transport of BB plumes. (B) Backward air parcel trajectory analysis of plumes arriving on the 16th of July (Stein et al., 2015). A larger image with higher resolution of the trajectory is presented in Figure S5. (C) Percent change of the mixing ratios of major VOCs measured during days with no wildfire event (July 12) and with significant transport of BB markers (July 16).*

Figure 5 shows a comparison of the VOC mixing ratios during the impact of wildfire plume (July 16) and non-BB event day (July 12), together with smoke mixing ratio observed at MOFLUX. Among the major VOCs, acetonitrile and benzene appeared to be associated with the transport of the wildfire plumes. These two VOCs had day average mixing ratios of 2.15 (acetonitrile) and 0.34 (benzene) ppb on July 16, corresponding to increases of 139% and 269%, respectively, compared to July 12, which is non-BB day. The major source of benzene shifted from vehicular

emissions to BB, highlighting the diverse activities influencing the variability of benzene at the temperate forest, as shown in the time series profile of benzene and Smoke (see Figure S6 in supplement).

3.4 Expanded List of VOCs and Their Response to Enhanced Temperature and Long-Range Transport of Wildfire Emissions

Beyond the major VOCs discussed above, more than 250 compounds with a mass to charge ratio (m/z) of at least 40 and with mixing ratios 5 ppt above the blank measurements were identified. The proposed molecular ion formulas are listed in Table S1. The compounds have a wide variety of molecular compositions, with maximums of 14, 23, 5, 3, and 2 numbers of carbon, hydrogen, oxygen, nitrogen, and sulfur, respectively, with a median formula of C_4H_6O and a mode of 2 degrees of unsaturation. The numbers of VOCs according to atomic content were as follows: 36 C_xH_y, 93 $C_xH_yO_w$, 17 $C_xH_yN_z$, 60, $C_xH_yO_wN_z$, and 10 $C_xH_yO_wS_v$, where v, y, x, y, and z are positive integers. The median oxygen-to-carbon ratio (O:C) and hydrogen-to-carbon ratio (H:C) of all the identified ions were 0.2 and 1.4. The O:C ratio was similar to a measurement in a boreal forest in southern Finland, which can be explained by the similarity of the measurement technique applied (i.e., Vocus PTR-ToF-MS), capturing fewer oxygenated compounds compared to other ionization techniques (i.e., Br and NO_3 instead of the hydronium ion) (Huang et al., 2021). The average log saturation vapor concentration for all the compounds was 7.50 μg m^{-3}, and 100 and 136 compounds were classified as intermediate and volatile organic compounds, respectively. Log C_{sat} values below 3 μg m^{-3} were recorded for three compounds (i.e., $C_6H_3NO_3$, $C_{10}H_{10}O_3$, and $C_{12}H_{23}NO_3$), which categorized them as semivolatile VOCs.

We analyzed July 8 through 17 to develop a deeper understanding of how the extended list of VOCs was influenced by both extreme heat and wildfire plumes. Note that in these analyses, the concentrations of acetone, isoprene, and MVK+MACr were not included to focus on the extended list of VOCs. During this period, the average VOC mixing ratio was 78 ppb with a standard deviation of 31.5. Figure 6 also shows the profile of the total VOC mixing ratios, which depicts a mixing ratio range between 23 to 147 ppb. Figure 6 illustrates the profiles of the weighted average of the O:C ratio, H:C ratio, and volatility of the VOCs. The O:C ratio was stable, ranging between 0.4 and 0.55. However, the apparent transport of the wildfire plume to the site decreased the ratio to less than 0.3 due to increase in reactive organic carbon. This is consistent with a prior study that reported a low O:C ratio (0.25) during intense biomass burning plume, compared to the measurement period when the smoke became diluted and impact of biogenic was emission enhanced (O:C =0.7) (Brito et al., 2014). The H:C ratio (1.8) was increased at the start period, characterized by low temperatures, which signifies the presence of highly unsaturated compounds such as aromatics. As the temperature increased, H:C values (1.5) decreased except during the period with BB emissions (1.75), implying the alteration of VOC distribution. Lastly, elevated temperature resulted in the emission of more volatile compounds, as the weighted average volatility reached 8.5 μg m^{-3}. The atmosphere over MOFLUX was further enriched with volatile compounds during the passage of the wildfire plume, as the mean log C_{sat} reached 9 μg m^{-3}.

Also in Figure 6 is the time series of the calculated OH reactivity during the intensive period influenced by extreme heat and wildfire plumes between July 8 to 17. Note that the calculation of reactivities included isoprene, acetone, and MVK+MACr. During this period, the average OH reactivity was 100.53 ± 10.79 s^{-1}, which was evidently higher

compared to previous measurements in urban environment in California, USA (Hansen et al., 2021), sub-urban site in Shanghai, China (Yang et al., 2022), and forest environments in Finland (Sinha et al., 2010) and France (Bsaibes et al., 2020). The elevated reactivity calculated in this study was attributed to the notable contributions from isoprene, acetone, ethylamine, and ethenone. To assess the impact of elevated temperatures and biomass burning on atmospheric reactivity, the data were categorized based on recorded ambient temperature and smoke concentration. The influence of biomass burning was evident from July 15 at 07:00 to July 17 at 20:00. Only one hour within this period had a temperature exceeding 32°C, and that data point was excluded from the average reactivity calculation. Conversely, the effect of extreme temperatures was evaluated using data recorded from July 8 at 01:00 to July 15 at 06:00. During this timeframe, 30 hours met the extreme temperature criteria (>32°C), allowing for an assessment of the potential impact of future warming on atmospheric reactivity. Periods with temperature conditions below 32°C that were not influenced by wildfire plumes were categorized as background. The average OH reactivities for periods with enhanced temperatures (>32 °C) and with transported plumes were 106.37 ± 4.27 s^{-1} and 106.22 ± 5.15 s^{-1}, respectively, both of which are substantially elevated compared to background conditions (98.78 ± 1.16 s^{-1}). The comparable OH reactivities of the two future climate scenarios highlight the reactive nature of biomass burning gas-phase species such as benzene and acetonitrile. Overall, the calculated averages during extreme heat and wildfires altered atmospheric reactivity in the forest.

Figure 7 shows the profile of the extended list of VOCs, clustered according to atomic content. The decreasing order of average concentration was as follows: $C_xH_yO_w$ (41 ppb), $C_xH_yO_wN_z$ (15 ppb), C_xH_y (11 ppb), $C_xH_yN_z$ (2.4 ppb), $C_xH_yO_wS_v$ (0.48 ppb). Hydrocarbons (C_xH_y) had evident enhancement at elevated temperature, as well as during the later hours of the transport of the BB compounds on the 16th of July. Oxygenated hydrocarbons ($C_xH_yO_w$) had a delayed response to temperature, in which peak concentration occurred around 18:00. Such categories also showed increased concentration during the initial hours of the wildfire plume arrival at MOFLUX. $C_xH_yN_z$ compounds such as acetonitrile showed clear augmentation during the initial hours of the plume transport but exhibited a less sensitive response to changes in temperature. For $C_xH_yO_wN_z$ and $C_xH_yO_wS_v$ compounds, temperature and BB had little to no effect on either group, except for the clear reduction during the latter hours of wildfire plume passage in the MOFLUX temperate forest.

Several compounds among the extended list showed an enhanced mixing ratio at high temperatures (>32°C). Besides the major compounds such as isoprene and monoterpene, VOCs such as formic acid (CH_2O_2, 8%), acetic acid ($C_2H_4O_2$, 83%), acrolein (C_3H_4O, 62%), furan (C_4H_4O, 62%, 51%), methylglyoxal ($C_3H_4O_2$, 51%), and glycolic acid ($C_2H_4O_3$, 68%) exhibited enhancement at the extreme temperature conditions, although it is equally possible that these compounds were also associated with transport of wildfire plumes. Values inside the parentheses are percent enhancement calculated using average concentrations at low (<32°C) and high (>32°C) temperature conditions. Formic and acetic acid, as two of the most dominant acids in the atmosphere, are key VOCs in aerosol growth, cloud precipitation, and rainwater acidity. Formic acid is primarily formed through photochemical production but can be emitted directly from vegetation, which is a temperature-dependent process (Millet et al., 2015).

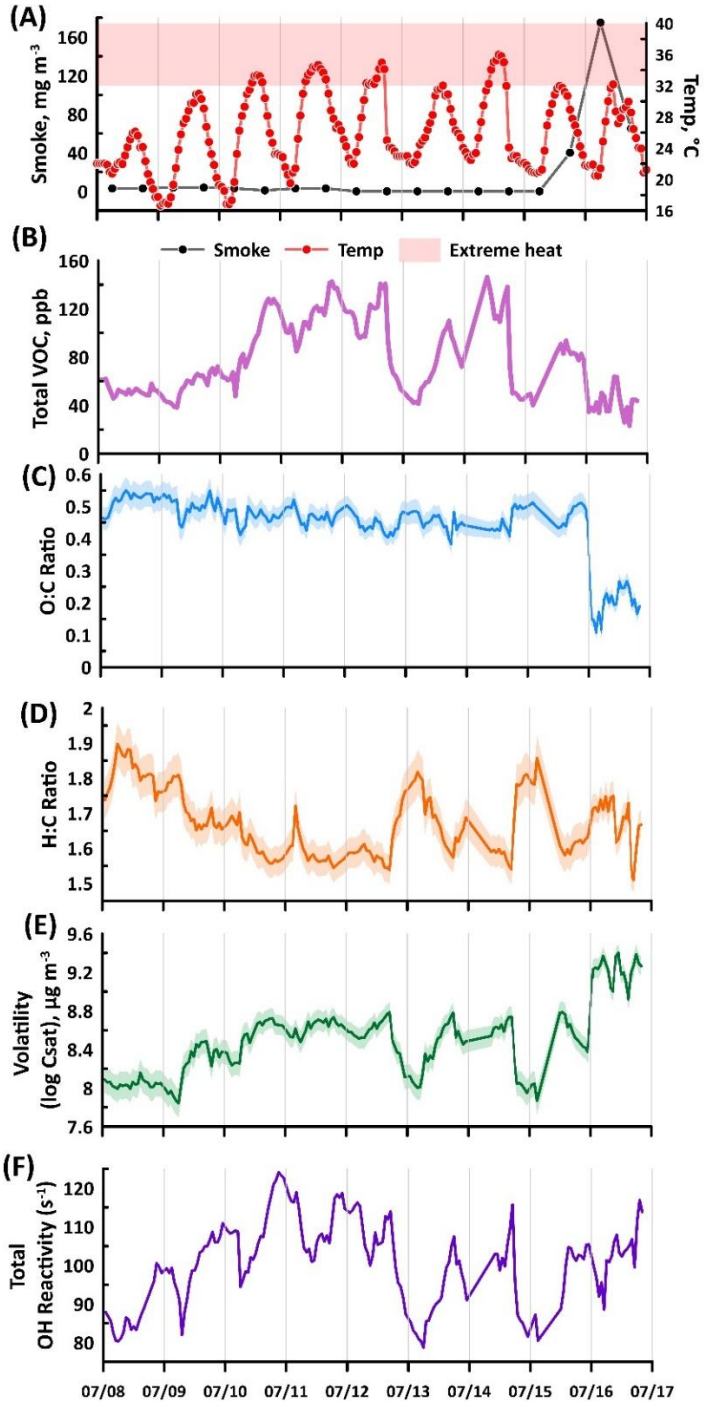

Figure 6. *(A) Time series profile of the smoke, and temperature observed at MOFLUX, (B) sum of VOC mixing ratio, (C) weighted O:C, (D) H:C ratios, (E) volatility, and (F) total reactivity during the intensive operational period between July 8 to 17. The shaded regions of O:C, H:C, and volatility are the weighted standard deviations.*

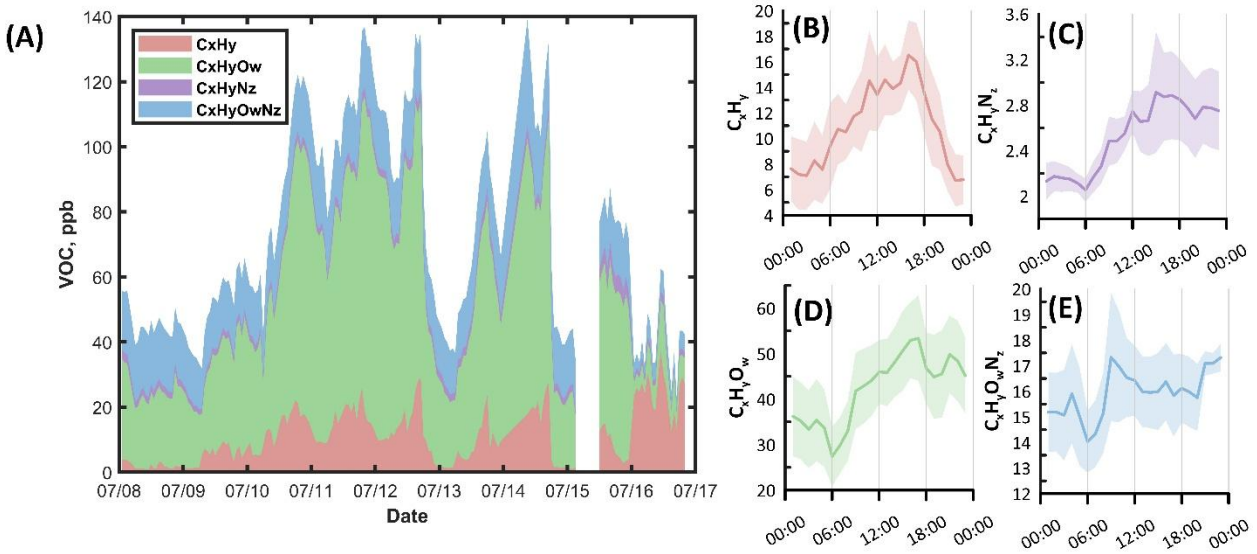

Figure 7. *(A) Time series and (B-E) diurnal profile of the clustering based on the atomic content of the VOCs during the intensive observation period with enhanced temperature and wildfire plume transport at MOFLUX. $C_xH_yO_wS_v$ compounds were not included due to low mixing ratio compared to other categories. Time series profile of the percent contribution of each VOC class is presented in Figure S7.*

3.5 Source Apportionment of VOCs Measured during Extreme Temperature and Biomass Burning

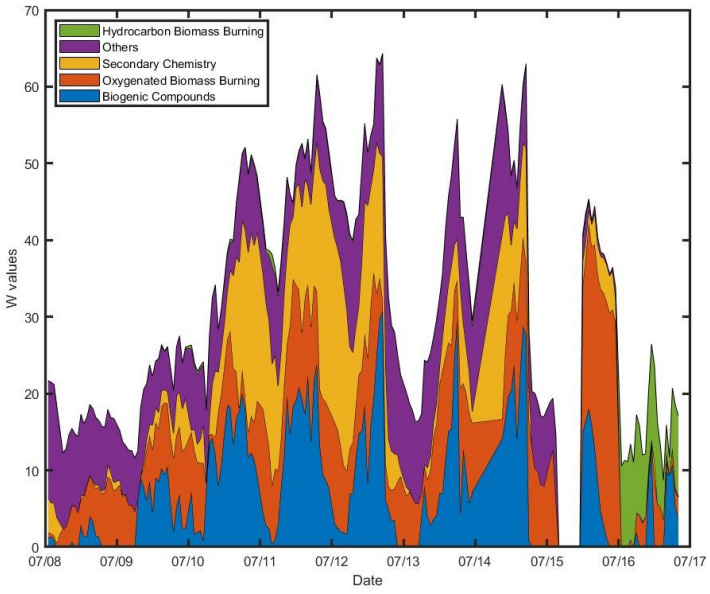

Figure 8. *Stacked profile of the non-negative factors of species fingerprints from all the VOCs measured at MOFLUX.*

To systematically investigate the pattern and contributions of the extended list of VOCs, a NNMF routine was applied to study the prominent sources of the VOCs in the forest between July 8 and 17. Based on the dominant tracers, response to the range of temperatures, impact of wildfire plume, and diurnal variations, five important categories were identified from the NNMF analysis: (i) Biogenic-related Compounds, (ii) Secondary Chemistry, (iii) Oxygenated BB compounds (O-BB), (iv) Hydrocarbon BB compounds (H-BB), and (v) Others. The "others" factor, with a substantial

number (N =137) of contributing compounds, remains unidentified. The time series of the factors are shown in Figure 8.

The biogenic factor, which consisted primarily of isoprene and monoterpene, followed the profile of temperature, which supports the attribution to biogenic sources. Two BB factors were accounted for, which were separated based on the chemical composition of the gases contributing to each factor. The median formulas for O-BB and H-BB were C_4H_5NO and C_6H_8, with a mode of 1 and 2 degrees of unsaturation, respectively. Pure hydrocarbons (C_xH_y) showed evident enhancement in the later hours of July 16. Also, the O-BB and H-BB factors are classified as volatile (log C_{sat} > 6 μg m^{-3}), based on the saturation mixing ratio values of 7.27 and 8.45 μg m^{-3}. The prominent compounds under the O-BB factor were acetonitrile (C_2H_3N), formamide (CH_3NO), maleic acid ($C_4H_4O_2$), hydroxyfuranone ($C_4H_4O_3$), butyramide or dimethylacetamide (C_4H_9NO), benzonitrile (C_7H_5N), and furaldehyde ($C_5H_5O_2$), which were all previously detected in field- and lab-scale measurements of wildfire plumes (Jain et al., 2023; Stockwell et al., 2015; Coggon et al., 2019; Salvador et al., 2022). The H-BB factor was populated by unsaturated hydrocarbons such as butadiene (C_4H_6), butene (C_4H_8), pentenes (C_5H_{10}), benzene (C_6H_6), hexadiene (C_6H_{10}), and ethylbenzene (C_8H_{10}), although cyclic hydrocarbons are not discounted. Interestingly, monoterpene at $C_{10}H_{17}^+$ and its fragment at $C_7H_8^+$ had substantial contributions from the H-BB factor during this period. The inclusion of monoterpenes in the H-BB factor is unlikely due to the expected biogenic emissions in the forest, even though the biogenic factor accounted for the second-largest contribution at 34%. However, several prior studies have shown that monoterpene can also originate from anthropogenic sources and wildfire events (Coggon et al., 2021), particularly BB events (Wang et al., 2022). With the enhancement of monoterpene and other unsaturated hydrocarbons (e.g., butenes and ethylbenzene) during wildfire plumes, several changes in atmospheric reactivity are expected, such as photochemical ozone production, scavenging of OH radicals, and suppression or enhancement of aerosol formation.

The secondary chemistry factor had a median chemical formula of $C_3H_4O_2$ with two degrees of unsaturation. Among the factors identified, this factor had the highest oxygen content, with a median and max of 2 and 5, respectively. Similar to the oxygenated hydrocarbon group, this factor had a diurnal profile characterized by evening enhancement (~20:00). Also, the secondary factor is marked by compounds such as ethenone (C_2H_2O), acrolein (C_3H_4O), acetic acid ($C_2H_4O_2$), MVK+MACr (C_4H_6O), hydroxyacetone ($C_3H_6O_2$), and acetylacetone ($C_5H_8O_2$). Isoprene also generates MVK during nighttime through the dominant β-RO_2 isomer formation pathway (Ng et al., 2017). During the transport of BB plumes, the secondary factor had a relatively low increase in signal compared to both BB factors, which shows that secondary formation was predominately locally generated with little to no contribution from long-range transport. BB tracers dominated the air mass of MOFLUX during the transport of the wildfire plume between July 15 and 17, which drastically affected the atmospheric chemistry of the area. This was corroborated by the enhanced reactivity (106.00 s^{-1}) during the transport of wildfire plume compared to background conditions (98.92 s^{-1}).

4. Summary and Conclusions

VOCs, which have important contributions to several atmospheric processes, were continuously measured in a temperate deciduous and juniper forest in the midwestern US during the summer of 2023 using PTR-ToF-MS. During the measurement period, the forest included several sources of biogenic compounds and was influenced by short- and long-range transport of anthropogenic and wildfire emissions. Extreme heat and wildfire emissions impacted the atmospheric conditions of the forest during the field measurement; such emissions are vital phenomena that provide insights into future climate. Typical VOCs, consisting of methanol, acetone, isoprene, monoterpene, MVK+MACr, benzene, toluene, acetonitrile, and catechol, had an average total mixing ratio of 69 ± 34 ppb .

Among the VOCs, isoprene had one of the highest recorded average mixing ratios (10 ± 9 ppb), next to methanol (23 ± 10 ppb) and acetone (22 ± 9 ppb). At the same time, monoterpene had three-fold enhancement at extreme temperatures. The large gap between the mixing ratios of isoprene and monoterpene suppressed the formation of aerosols due to the scavenging of OH radicals and reduction of C_{20} dimers. AVOCs such as benzene (0.42 ppb) and acetonitrile (1.52 ppb) responded much less to changes in temperature compared to the BVOCs. The varying enrichment of the major VOCs and their response to extreme temperatures influenced the atmospheric reactivity in the temperate forest. New studies indicated that the coexistence of multiple precursor VOCs can generate unexplored molecular-scale interactions, which is critical as current and future VOC distributions are expected to be widely different compared to current conditions. For instance, the coexistence of isoprene and monoterpene led to reduced hydroxyl radical availability, leading to a limited oxidation process (Mcfiggans et al., 2019).

Besides the role of elevated temperature, the duration of the VOC measurement at MOFLUX was marked by sporadic transport of plumes from wildfires in Canada. The impending warming of the atmosphere is projected to potentially increase the frequency and duration of wildfires due to drier seasons. In MOFLUX, the profiles of the major VOCs such as benzene and acetonitrile changed notably with respect to the wildfire plumes, as their concentrations were enhanced by more than 100%. As benzene is a crucial precursor for ozone and a significant contributor to aerosol formation, the variability of such BB VOC should be incorporated into simulations of future atmospheric processes.

Beyond the major VOCs, analysis of the whole mass spectra revealed more than 250 other compounds, the mixing ratios of which sum to as much as 78 ppb during a period with elevated temperature (>32 °C) and BB plumes (smoke > 100 mg m^{-3}). With a similar mixing ratio sum to those of the VOCs, analysis of unaccounted-for VOCs is necessary to perform a realistic investigation of the relevant atmospheric processes at the MOFLUX site. The O:C and H:C ratios of the measured VOCs, as well as their volatility, provided insight into their response to future climate scenarios. During BB plume transport, hydrocarbons (C_xH_y) with high volatility were enhanced. C_xH_y and $C_xH_yN_z$ compounds dominated the total VOC mixing ratio during the initial and later hours of biomass transport, respectively, whereas oxygenated hydrocarbons persisted consistently during periods of elevated temperature. Furthermore, the analysis of the entire spectra pinpointed an additional 40 compounds that have at least 100% enhancement in mixing ratio at

564 extreme temperatures and/or during the transport of wildfire emissions. Two of them are formic (0.89 ppb) and acetic
565 acid (3.29 ppb), which have a vital impact on atmospheric acidity and cloud formation.
566
567 The highly variable profiles of the extended list of VOCs measured at MOFLUX indicated that species were impacted
568 by a variety of emissions and processes. NNMF was applied to the VOC mixing ratios, and five factors were identified:
569 two BB factors and one each for secondary chemistry, biogenic, and others. The two BB factors were resolved based
570 on the chemical composition of the compounds contributing to each factor. With the high reactivity of such compounds
571 to OH radicals, it is expected that BB altered the normal forest-dominated atmospheric processes.
572

Data availability

The data used in this publication are available to the community and can be accessed in ORNL's Terrestrial Ecosystem Science Scientific Focus Area - Data Products and Tools website under the Volatile Organic Compounds and Meteorological Conditions in the Missouri Ozark AmeriFlux (MOFLUX) Site, 2023 data product which can be accessed via the DOI: https://doi.org/10.25581/ornlsfa.033/2409393

Author contribution:

CMS, JDW, EGC, HAS, BDK, and SSO conducted the measurements. CMS, JDW, MAM, KRB, and LG designed the project, coordinated the measurements, and supervised the study. MAM, LG, and KRB obtained funding for the project. CMS and KRB carried out data curation and analysis. CMS prepared the manuscript. All co-authors contributed to the discussion and the interpretation of the results.

Competing interests:

The authors declare that they have no conflict of interest.

Acknowledgements

This research was funded through Oak Ridge National Laboratory (ORNL)'s Directed Research and Development (LDRD) program. ORNL is managed by the University of Tennessee-Battelle, LLC, under contract DE-AC05-00OR22725 with the U.S. Department of Energy. The U.S. Drought Monitor, which provided the drought data of Boone County, MO, is jointly produced by the National Drought Mitigation Center at the University of Nebraska-Lincoln, the United States Department of Agriculture, and the National Oceanic and Atmospheric Administration. The authors gratefully acknowledge the NOAA Air Resources Laboratory (ARL) for the provision of the HYSPLIT transport and dispersion model (https://www.ready.noaa.gov) used in this publication.

REFERENCES

Ambrose, J. L., Haase, K., Russo, R. S., Zhou, Y., White, M. L., Frinak, E. K., Jordan, C., Mayne, H. R., Talbot, R., and Sive, B. C.: A comparison of GC-FID and PTR-MS toluene measurements in ambient air under conditions of enhanced monoterpene loading, Atmos. Meas. Tech., 3, 959-980, 10.5194/amt-3-959-2010, 2010.

Bates, K. H., Jacob, D. J., Wang, S., Hornbrook, R. S., Apel, E. C., Kim, M. J., Millet, D. B., Wells, K. C., Chen, X., Brewer, J. F., Ray, E. A., Commane, R., Diskin, G. S., and Wofsy, S. C.: The Global Budget of Atmospheric Methanol: New Constraints on Secondary, Oceanic, and Terrestrial Sources, J. Geophys. Res. Atmos., 126, e2020JD033439, https://doi.org/10.1029/2020JD033439, 2021.

Blake, R. S., Monks, P. S., and Ellis, A. M.: Proton-Transfer Reaction Mass Spectrometry, Chem. Rev., 109, 861-896, 10.1021/cr800364q, 2009.

Binte Shahid, S., Lacey, F. G., Wiedinmyer, C., Yokelson, R. J., and Barsanti, K. C.: NEIVAv1.0: Next-generation Emissions InVentory expansion of Akagi et al. (2011) version 1.0, Geosci. Model Dev., 17, 7679-7711, 10.5194/gmd-17-7679-2024, 2024.

Bourgeois, I., Peischl, J., Neuman, J. A., Brown, S. S., Thompson, C. R., Aikin, K. C., Allen, H. M., Angot, H., Apel, E. C., Baublitz, C. B., Brewer, J. F., Campuzano-Jost, P., Commane, R., Crounse, J. D., Daube, B. C., DiGangi, J. P., Diskin, G. S., Emmons, L. K., Fiore, A. M., Gkatzelis, G. I., Hills, A., Hornbrook, R. S., Huey, L. G., Jimenez, J. L., Kim, M., Lacey, F., McKain, K., Murray, L. T., Nault, B. A., Parrish, D. D., Ray, E., Sweeney, C., Tanner, D., Wofsy, S. C., and Ryerson, T. B.: Large contribution of biomass burning emissions to ozone throughout the global remote troposphere, Proc. Natl. Acad. Sci., 118, e2109628118, doi:10.1073/pnas.2109628118, 2021.

Brito, J., Rizzo, L. V., Morgan, W. T., Coe, H., Johnson, B., Haywood, J., Longo, K., Freitas, S., Andreae, M. O., and Artaxo, P.: Ground-based aerosol characterization during the South American Biomass Burning Analysis (SAMBBA) field experiment, Atmos. Chem. Phys., 14, 12069-12083, 10.5194/acp-14-12069-2014, 2014.

Bsaibes, S., Al Ajami, M., Mermet, K., Truong, F., Batut, S., Hecquet, C., Dusanter, S., Léornadis, T., Sauvage, S., Kammer, J., Flaud, P. M., Perraudin, E., Villenave, E., Locoge, N., Gros, V., and Schoemaecker, C.: Variability of hydroxyl radical (OH) reactivity in the Landes maritime pine forest: results from the LANDEX campaign 2017, Atmos. Chem. Phys., 20, 1277-1300, 10.5194/acp-20-1277-2020, 2020.

Byrne, B., Liu, J., Bowman, K., Pascolini-Campbell, M., Chatterjee, A., Pandey, S., Miyazaki, K., van der Werf, G., Wunch, D., and Wennberg, P.: Unprecedented Canadian forest fire carbon emissions during 2023, 2023.

Chen, T., Zhang, P., Chu, B., Ma, Q., Ge, Y., Liu, J., and He, H.: Secondary organic aerosol formation from mixed volatile organic compounds: Effect of RO2 chemistry and precursor concentration, npj Climate and Atmospheric Science, 5, 95, 10.1038/s41612-022-00321-y, 2022.

Ciccioli, P., Centritto, M., and Loreto, F.: Biogenic volatile organic compound emissions from vegetation fires, Plant, Cell & Environment, 37, 1810-1825, https://doi.org/10.1111/pce.12336, 2014.

Chow, F. K., Yu, K. A., Young, A., James, E., Grell, G. A., Csiszar, I., Tsidulko, M., Freitas, S., Pereira, G., Giglio, L., Friberg, M. D., and Ahmadov, R.: High-Resolution Smoke Forecasting for the 2018 Camp Fire in

California, Bulletin of the American Meteorological Society, 103, E1531-E1552, https://doi.org/10.1175/BAMS-D-20-0329.1, 2022.

Coggon, M. M., Lim, C. Y., Koss, A. R., Sekimoto, K., Yuan, B., Gilman, J. B., Hagan, D. H., Selimovic, V., Zarzana, K. J., Brown, S. S., Roberts, J. M., Müller, M., Yokelson, R., Wisthaler, A., Krechmer, J. E., Jimenez, J. L., Cappa, C., Kroll, J. H., de Gouw, J., and Warneke, C.: OH chemistry of non-methane organic gases (NMOGs) emitted from laboratory and ambient biomass burning smoke: evaluating the influence of furans and oxygenated aromatics on ozone and secondary NMOG formation, Atmos. Chem. Phys., 19, 14875-14899, 10.5194/acp-19-14875-2019, 2019.

Coggon, M. M., Gkatzelis, G. I., McDonald, B. C., Gilman, J. B., Schwantes, R. H., Abuhassan, N., Aikin, K. C., Arend, M. F., Berkoff, T. A., Brown, S. S., Campos, T. L., Dickerson, R. R., Gronoff, G., Hurley, J. F., Isaacman-VanWertz, G., Koss, A. R., Li, M., McKeen, S. A., Moshary, F., Peischl, J., Pospisilova, V., Ren, X., Wilson, A., Wu, Y., Trainer, M., and Warneke, C.: Volatile chemical product emissions enhance ozone and modulate urban chemistry, Proc. Natl. Acad. Sci., 118, e2026653118, doi:10.1073/pnas.2026653118, 2021.

Collins, M., Knutti, R., Arblaster, J., Dufresne, J.-L., Fichefet, T., Friedlingstein, P., Gao, X., Gutowski, W. J., Johns, T., and Krinner, G.: Long-term climate change: projections, commitments and irreversibility, 2013.

Daussy, J. and Staudt, M.: Do future climate conditions change volatile organic compound emissions from Artemisia annua? Elevated CO2 and temperature modulate actual VOC emission rate but not its emission capacity, Atmospheric Environment: X, 7, 100082, https://doi.org/10.1016/j.aeaoa.2020.100082, 2020.

Donahue, N. M., Epstein, S. A., Pandis, S. N., and Robinson, A. L.: A two-dimensional volatility basis set: 1. organic-aerosol mixing thermodynamics, Atmos. Chem. Phys., 11, 3303-3318, 10.5194/acp-11-3303-2011, 2011.

Duncan, B. N., Yoshida, Y., Damon, M. R., Douglass, A. R., and Witte, J. C.: Temperature dependence of factors controlling isoprene emissions, Geophysical Research Letters, 36, https://doi.org/10.1029/2008GL037090, 2009.

Ferracci, V., Bolas, C. G., Freshwater, R. A., Staniaszek, Z., King, T., Jaars, K., Otu-Larbi, F., Beale, J., Malhi, Y., Waine, T. W., Jones, R. L., Ashworth, K., and Harris, N. R. P.: Continuous Isoprene Measurements in a UK Temperate Forest for a Whole Growing Season: Effects of Drought Stress During the 2018 Heatwave, Geophysical Research Letters, 47, e2020GL088885, https://doi.org/10.1029/2020GL088885, 2020.

Finewax, Z., de Gouw, J. A., and Ziemann, P. J.: Identification and Quantification of 4-Nitrocatechol Formed from OH and NO3 Radical-Initiated Reactions of Catechol in Air in the Presence of NOx: Implications for Secondary Organic Aerosol Formation from Biomass Burning, Environ. Sci. Technol., 52, 1981-1989, 10.1021/acs.est.7b05864, 2018.

Fuentes, J. D. and Wang, D.: ON THE SEASONALITY OF ISOPRENE EMISSIONS FROM A MIXED TEMPERATE FOREST, Ecological Applications, 9, 1118-1131, https://doi.org/10.1890/1051-0761(1999)009[1118:OTSOIE]2.0.CO;2, 1999.

Geron, C., Daly, R., Harley, P., Rasmussen, R., Seco, R., Guenther, A., Karl, T., and Gu, L.: Large drought-induced variations in oak leaf volatile organic compound emissions during PINOT NOIR 2012, Chemosphere, 146, 8-21, https://doi.org/10.1016/j.chemosphere.2015.11.086, 2016.

Gilman, J. B., Lerner, B. M., Kuster, W. C., Goldan, P. D., Warneke, C., Veres, P. R., Roberts, J. M., de Gouw, J. A., Burling, I. R., and Yokelson, R. J.: Biomass burning emissions and potential air quality impacts of volatile organic compounds and other trace gases from fuels common in the US, Atmos. Chem. Phys., 15, 13915-13938, 10.5194/acp-15-13915-2015, 2015.

Greenberg, J. P., Guenther, A. B., Pétron, G., Wiedinmyer, C., Vega, O., Gatti, L. V., Tota, J., and Fisch, G.: Biogenic VOC emissions from forested Amazonian landscapes, Global Change Biology, 10, 651-662, https://doi.org/10.1111/j.1365-2486.2004.00758.x, 2004.

Gu, L., Pallardy, S. G., Hosman, K. P., and Sun, Y.: Drought-influenced mortality of tree species with different predawn leaf water dynamics in a decade-long study of a central US forest, Biogeosciences, 12, 2831-2845, 10.5194/bg-12-2831-2015, 2015.

Guenther, A. B., Jiang, X., Heald, C. L., Sakulyanontvittaya, T., Duhl, T., Emmons, L. K., and Wang, X.: The Model of Emissions of Gases and Aerosols from Nature version 2.1 (MEGAN2.1): an extended and updated framework for modeling biogenic emissions, Geosci. Model Dev., 5, 1471-1492, 10.5194/gmd-5-1471-2012, 2012.

Guenther, A. B., Zimmerman, P. R., Harley, P. C., Monson, R. K., and Fall, R.: Isoprene and monoterpene emission rate variability: model evaluations and sensitivity analyses, J. Geophys. Res. Atmos., 98, 12609-12617, 1993.

Hakola, H., Hellén, H., Hemmilä, M., Rinne, J., and Kulmala, M.: In situ measurements of volatile organic compounds in a boreal forest, Atmos. Chem. Phys., 12, 11665-11678, 10.5194/acp-12-11665-2012, 2012.

Hallquist, M., Wenger, J. C., Baltensperger, U., Rudich, Y., Simpson, D., Claeys, M., Dommen, J., Donahue, N. M., George, C., Goldstein, a. H., Hamilton, J. F., Herrmann, H., Hoffmann, T., Iinuma, Y., Jang, M., Jenkin, M. E., Jimenez, J. L., Kiendler-Scharr, a., Maenhaut, W., McFiggans, G., Mentel, T. F., Monod, a., Prévôt, a. S. H., Seinfeld, J. H., Surratt, J. D., Szmigielski, R., and Wildt, J.: The formation, properties and impact of secondary organic aerosol: current and emerging issues, Atmos. Chem. Phys., 9, 5155-5236, 10.5194/acp-9-5155-2009, 2009.

Hansen, R. F., Griffith, S. M., Dusanter, S., Gilman, J. B., Graus, M., Kuster, W. C., Veres, P. R., de Gouw, J. A., Warneke, C., Washenfelder, R. A., Young, C. J., Brown, S. S., Alvarez, S. L., Flynn, J. H., Grossberg, N. E., Lefer, B., Rappenglueck, B., and Stevens, P. S.: Measurements of Total OH Reactivity During CalNex-LA, J. Geophys. Res. Atmos., 126, e2020JD032988, https://doi.org/10.1029/2020JD032988, 2021.

Hatch, L. E., Luo, W., Pankow, J. F., Yokelson, R. J., Stockwell, C. E., and Barsanti, K. C.: Identification and quantification of gaseous organic compounds emitted from biomass burning using two-dimensional gas chromatography–time-of-flight mass spectrometry, Atmos. Chem. Phys., 15, 1865-1899, 10.5194/acp-15-1865-2015, 2015.

Heiden, A. C., Kobel, K., Komenda, M., Koppmann, R., Shao, M., and Wildt, J.: Toluene emissions from plants, Geophysical Research Letters, 26, 1283-1286, https://doi.org/10.1029/1999GL900220, 1999.

Heinritzi, M., Dada, L., Simon, M., Stolzenburg, D., Wagner, A. C., Fischer, L., Ahonen, L. R., Amanatidis, S., Baalbaki, R., Baccarini, A., Bauer, P. S., Baumgartner, B., Bianchi, F., Brilke, S., Chen, D., Chiu, R., Dias, A., Dommen, J., Duplissy, J., Finkenzeller, H., Frege, C., Fuchs, C., Garmash, O., Gordon, H., Granzin, M., El Haddad, I., He, X., Helm, J., Hofbauer, V., Hoyle, C. R., Kangasluoma, J., Keber, T., Kim, C., Kürten, A., Lamkaddam, H., Laurila, T. M., Lampilahti, J., Lee, C. P., Lehtipalo, K., Leiminger, M., Mai, H., Makhmutov, V., Manninen, H. E., Marten, R., Mathot, S., Mauldin, R. L., Mentler, B., Molteni, U., Müller, T., Nie, W., Nieminen, T., Onnela, A., Partoll, E., Passananti, M., Petäjä, T., Pfeifer, J., Pospisilova, V., Quéléver, L. L. J., Rissanen, M. P., Rose, C., Schobesberger, S., Scholz, W., Scholze, K., Sipilä, M., Steiner, G., Stozhkov, Y., Tauber, C., Tham, Y. J., Vazquez-Pufleau, M., Virtanen, A., Vogel, A. L., Volkamer, R., Wagner, R., Wang, M., Weitz, L., Wimmer, D., Xiao, M., Yan, C., Ye, P., Zha, Q., Zhou, X., Amorim, A., Baltensperger, U., Hansel, A., Kulmala, M., Tomé, A., Winkler, P. M., Worsnop, D. R., Donahue, N. M., Kirkby, J., and Curtius, J.: Molecular understanding of the suppression of new-particle formation by isoprene, Atmos. Chem. Phys., 20, 11809-11821, 10.5194/acp-20-11809-2020, 2020.

Hu, L., Millet, D. B., Baasandorj, M., Griffis, T. J., Turner, P., Helmig, D., Curtis, A. J., and Hueber, J.: Isoprene emissions and impacts over an ecological transition region in the U.S. Upper Midwest inferred from tall tower measurements, J. Geophys. Res. Atmos., 120, 3553-3571, https://doi.org/10.1002/2014JD022732, 2015.

Hu, L., Millet, D. B., Kim, S. Y., Wells, K. C., Griffis, T. J., Fischer, E. V., Helmig, D., Hueber, J., and Curtis, A. J.: North American acetone sources determined from tall tower measurements and inverse modeling, Atmos. Chem. Phys., 13, 3379-3392, 10.5194/acp-13-3379-2013, 2013.

Huang, W., Li, H., Sarnela, N., Heikkinen, L., Tham, Y. J., Mikkilä, J., Thomas, S. J., Donahue, N. M., Kulmala, M., and Bianchi, F.: Measurement report: Molecular composition and volatility of gaseous organic compounds in a boreal forest – from volatile organic compounds to highly oxygenated organic molecules, Atmos. Chem. Phys., 21, 8961-8977, 10.5194/acp-21-8961-2021, 2021.

Huangfu, Y., Yuan, B., Wang, S., Wu, C., He, X., Qi, J., de Gouw, J., Warneke, C., Gilman, J. B., Wisthaler, A., Karl, T., Graus, M., Jobson, B. T., and Shao, M.: Revisiting Acetonitrile as Tracer of Biomass Burning in Anthropogenic-Influenced Environments, Geophysical Research Letters, 48, e2020GL092322, https://doi.org/10.1029/2020GL092322, 2021.

Jain, V., Tripathi, N., Tripathi, S. N., Gupta, M., Sahu, L. K., Murari, V., Gaddamidi, S., Shukla, A. K., and Prevot, A. S. H.: Real-time measurements of non-methane volatile organic compounds in the central Indo-Gangetic basin, Lucknow, India: source characterisation and their role in O3 and secondary organic aerosol formation, Atmos. Chem. Phys., 23, 3383-3408, 10.5194/acp-23-3383-2023, 2023.

Jardine, K. J., Jardine, A. B., Holm, J. A., Lombardozzi, D. L., Negron-Juarez, R. I., Martin, S. T., Beller, H. R., Gimenez, B. O., Higuchi, N., and Chambers, J. Q.: Monoterpene 'thermometer' of tropical forest-atmosphere response to climate warming, Plant, Cell & Environment, 40, 441-452, https://doi.org/10.1111/pce.12879, 2017.

Jardine, K. J., Chambers, J. Q., Holm, J., Jardine, A. B., Fontes, C. G., Zorzanelli, R. F., Meyers, K. T., De Souza, V. F., Garcia, S., Gimenez, B. O., Piva, L. R. d. O., Higuchi, N., Artaxo, P., Martin, S., and Manzi, A. O.: Green

Leaf Volatile Emissions during High Temperature and Drought Stress in a Central Amazon Rainforest, Plants, 4, 678-690, 2015.

Jin, L., Permar, W., Selimovic, V., Ketcherside, D., Yokelson, R. J., Hornbrook, R. S., Apel, E. C., Ku, I. T., Collett Jr, J. L., Sullivan, A. P., Jaffe, D. A., Pierce, J. R., Fried, A., Coggon, M. M., Gkatzelis, G. I., Warneke, C., Fischer, E. V., and Hu, L.: Constraining emissions of volatile organic compounds from western US wildfires with WE-CAN and FIREX-AQ airborne observations, Atmos. Chem. Phys., 23, 5969-5991, 10.5194/acp-23-59-2023, 2023.

Juang, C. S., Williams, A. P., Abatzoglou, J. T., Balch, J. K., Hurteau, M. D., and Moritz, M. A.: Rapid Growth of Large Forest Fires Drives the Exponential Response of Annual Forest-Fire Area to Aridity in the Western United States, Geophysical Research Letters, 49, e2021GL097131, https://doi.org/10.1029/2021GL097131, 2022.

Kanawade, V. P., Jobson, B. T., Guenther, A. B., Erupe, M. E., Pressley, S. N., Tripathi, S. N., and Lee, S. H.: Isoprene suppression of new particle formation in a mixed deciduous forest, Atmos. Chem. Phys., 11, 6013-6027, 10.5194/acp-11-6013-2011, 2011.

Ketcherside, D. T., Miller, D. D., Kenerson, D. R., Scott, P. S., Andrew, J. P., Bakker, M. A. Y., Bundy, B. A., Grimm, B. K., Li, J., Nuñez, L. A., Pittman, D. L., Uhlorn, R. P., and Johnston, N. A. C.: Effects of Wildfire Smoke on Volatile Organic Compound (VOC) and PM2.5 Composition in a United States Intermountain Western Valley and Estimation of Human Health Risk, Atmosphere, 15, 1172, 2024.

Kiendler-Scharr, A., Wildt, J., Maso, M. D., Hohaus, T., Kleist, E., Mentel, T. F., Tillmann, R., Uerlings, R., Schurr, U., and Wahner, A.: New particle formation in forests inhibited by isoprene emissions, Nature, 461, 381-384, http://www.nature.com/nature/journal/v461/n7262/suppinfo/nature08292_S1.html, 2009.

Koss, A. R., Sekimoto, K., Gilman, J. B., Selimovic, V., Coggon, M. M., Zarzana, K. J., Yuan, B., Lerner, B. M., Brown, S. S., Jimenez, J. L., Krechmer, J., Roberts, J. M., Warneke, C., Yokelson, R. J., and de Gouw, J.: Non-methane organic gas emissions from biomass burning: identification, quantification, and emission factors from PTR-ToF during the FIREX 2016 laboratory experiment, Atmos. Chem. Phys., 18, 3299-3319, 10.5194/acp-18-3299-2018, 2018.

Kumar, V., Chandra, B. P., and Sinha, V.: Large unexplained suite of chemically reactive compounds present in ambient air due to biomass fires, Scientific Reports, 8, 626, 10.1038/s41598-017-19139-3, 2018.

Lantz, A. T., Allman, J., Weraduwage, S. M., and Sharkey, T. D.: Control of rate and physiological role of isoprene emission from plants, Plant, cell & environment, 42, 2808, 2019a.

Lantz, A. T., Solomon, C., Gog, L., McClain, A. M., Weraduwage, S. M., Cruz, J. A., and Sharkey, T. D.: Isoprene Suppression by CO2 Is Not Due to Triose Phosphate Utilization (TPU) Limitation, Frontiers in Forests and Global Change, 2, 10.3389/ffgc.2019.00008, 2019b.

Lee, J.-Y., Marotzke, J., Bala, G., Cao, L., Corti, S., Dunne, J. P., Engelbrecht, F., Fischer, E., Fyfe, J. C., and Jones, C.: Future global climate: scenario-based projections and near-term information, in: Climate change 2021: The physical science basis. Contribution of working group I to the sixth assessment report of the intergovernmental panel on climate change, Cambridge University Press, 553-672, 2021.

Lee, S.-H., Uin, J., Guenther, A. B., de Gouw, J. A., Yu, F., Nadykto, A. B., Herb, J., Ng, N. L., Koss, A., Brune, W. H., Baumann, K., Kanawade, V. P., Keutsch, F. N., Nenes, A., Olsen, K., Goldstein, A., and Ouyang, Q.: Isoprene suppression of new particle formation: Potential mechanisms and implications, J. Geophys. Res. Atmos., 121, 14,621-614,635, https://doi.org/10.1002/2016JD024844, 2016.

Li, L., Tang, P., Nakao, S., Chen, C. L., and Cocker Iii, D. R.: Role of methyl group number on SOA formation from monocyclic aromatic hydrocarbons photooxidation under low-NOx conditions, Atmos. Chem. Phys., 16, 2255-2272, 10.5194/acp-16-2255-2016, 2016.

Liang, Y., Stamatis, C., Fortner, E. C., Wernis, R. A., Van Rooy, P., Majluf, F., Yacovitch, T. I., Daube, C., Herndon, S. C., Kreisberg, N. M., Barsanti, K. C., and Goldstein, A. H.: Emissions of organic compounds from western US wildfires and their near-fire transformations, Atmos. Chem. Phys., 22, 9877-9893, 10.5194/acp-22-9877-2022, 2022.

Ling, Z., He, Z., Wang, Z., Shao, M., and Wang, X.: Sources of methacrolein and methyl vinyl ketone and their contributions to methylglyoxal and formaldehyde at a receptor site in Pearl River Delta, Journal of Environmental Sciences, 79, 1-10, https://doi.org/10.1016/j.jes.2018.12.001, 2019.

Loreto, F. and Schnitzler, J.-P.: Abiotic stresses and induced BVOCs, Trends in plant science, 15, 154-166, 2010.

Malik, T. G., Gajbhiye, T., and Pandey, S. K.: Some insights into composition and monoterpene emission rates from selected dominant tropical tree species of Central India: Plant-specific seasonal variations, Ecological Research, 34, 821-834, 2019.

Malik, T. G., Sahu, L. K., Gupta, M., Mir, B. A., Gajbhiye, T., Dubey, R., Clavijo McCormick, A., and Pandey, S. K.: Environmental Factors Affecting Monoterpene Emissions from Terrestrial Vegetation, Plants, 12, 3146, 2023.

McFiggans, G., Mentel, T. F., Wildt, J., Pullinen, I., Kang, S., Kleist, E., Schmitt, S., Springer, M., Tillmann, R., Wu, C., Zhao, D., Hallquist, M., Faxon, C., Le Breton, M., Hallquist, Å. M., Simpson, D., Bergström, R., Jenkin, M. E., Ehn, M., Thornton, J. A., Alfarra, M. R., Bannan, T. J., Percival, C. J., Priestley, M., Topping, D., and Kiendler-Scharr, A.: Secondary organic aerosol reduced by mixture of atmospheric vapours, Nature, 565, 587-593, 10.1038/s41586-018-0871-y, 2019.

McGlynn, D. F., Frazier, G., Barry, L. E. R., Lerdau, M. T., Pusede, S. E., and Isaacman-VanWertz, G.: Minor contributions of daytime monoterpenes are major contributors to atmospheric reactivity, Biogeosciences, 20, 45-55, 10.5194/bg-20-45-2023, 2023.

Millet, D. B., Baasandorj, M., Farmer, D. K., Thornton, J. A., Baumann, K., Brophy, P., Chaliyakunnel, S., de Gouw, J. A., Graus, M., Hu, L., Koss, A., Lee, B. H., Lopez-Hilfiker, F. D., Neuman, J. A., Paulot, F., Peischl, J., Pollack, I. B., Ryerson, T. B., Warneke, C., Williams, B. J., and Xu, J.: A large and ubiquitous source of atmospheric formic acid, Atmos. Chem. Phys., 15, 6283-6304, 10.5194/acp-15-6283-2015, 2015.

Mohr, C., Thornton, J. A., Heitto, A., Lopez-Hilfiker, F. D., Lutz, A., Riipinen, I., Hong, J., Donahue, N. M., Hallquist, M., Petäjä, T., Kulmala, M., and Yli-Juuti, T.: Molecular identification of organic vapors driving atmospheric nanoparticle growth, Nature Communications, 10, 4442, 10.1038/s41467-019-12473-2, 2019.

Montzka, S. A., Trainer, M., Angevine, W. M., and Fehsenfeld, F. C.: Measurements of 3-methyl furan, methyl vinyl ketone, and methacrolein at a rural forested site in the southeastern United States, J. Geophys. Res. Atmos., 100, 11393-11401, https://doi.org/10.1029/95JD01132, 1995.

Nagalingam, S., Seco, R., Kim, S., and Guenther, A.: Heat stress strongly induces monoterpene emissions in some plants with specialized terpenoid storage structures, Agricultural and Forest Meteorology, 333, 109400, https://doi.org/10.1016/j.agrformet.2023.109400, 2023.

Navarro, M. A., Dusanter, S., and Stevens, P. S.: Temperature dependence of the yields of methacrolein and methyl vinyl ketone from the OH-initiated oxidation of isoprene under NOx-free conditions, Atmos. Environ., 79, 59-66, https://doi.org/10.1016/j.atmosenv.2013.06.032, 2013.

Ng, N. L., Kroll, J. H., Chan, A. W. H., Chhabra, P. S., Flagan, R. C., and Seinfeld, J. H.: Secondary organic aerosol formation from m-xylene, toluene, and benzene, Atmos. Chem. Phys., 7, 3909-3922, 10.5194/acp-7-3909-2007, 2007.

Ng, N. L., Brown, S. S., Archibald, A. T., Atlas, E., Cohen, R. C., Crowley, J. N., Day, D. A., Donahue, N. M., Fry, J. L., Fuchs, H., Griffin, R. J., Guzman, M. I., Herrmann, H., Hodzic, A., Iinuma, Y., Jimenez, J. L., Kiendler-Scharr, A., Lee, B. H., Luecken, D. J., Mao, J., McLaren, R., Mutzel, A., Osthoff, H. D., Ouyang, B., Picquet-Varrault, B., Platt, U., Pye, H. O. T., Rudich, Y., Schwantes, R. H., Shiraiwa, M., Stutz, J., Thornton, J. A., Tilgner, A., Williams, B. J., and Zaveri, R. A.: Nitrate radicals and biogenic volatile organic compounds: oxidation, mechanisms, and organic aerosol, Atmos. Chem. Phys., 17, 2103-2162, 10.5194/acp-17-2103-2017, 2017.

Park, S., Allen, R. J., and Lim, C. H.: A likely increase in fine particulate matter and premature mortality under future climate change, Air Quality, Atmosphere & Health, 13, 143-151, 10.1007/s11869-019-00785-7, 2020.

Patiny, L. and Borel, A.: ChemCalc: A Building Block for Tomorrow's Chemical Infrastructure, Journal of Chemical Information and Modeling, 53, 1223-1228, 10.1021/ci300563h, 2013.

Perkins-Kirkpatrick, S. E. and Gibson, P. B.: Changes in regional heatwave characteristics as a function of increasing global temperature, Scientific Reports, 7, 12256, 10.1038/s41598-017-12520-2, 2017.

Perkins, S. E. and Alexander, L. V.: On the measurement of heat waves, Journal of climate, 26, 4500-4517, 2013.

Permar, W., Jin, L., Peng, Q., O'Dell, K., Lill, E., Selimovic, V., Yokelson, R. J., Hornbrook, R. S., Hills, A. J., Apel, E. C., Ku, I. T., Zhou, Y., Sive, B. C., Sullivan, A. P., Collett, J. L., Palm, B. B., Thornton, J. A., Flocke, F., Fischer, E. V., and Hu, L.: Atmospheric OH reactivity in the western United States determined from comprehensive gas-phase measurements during WE-CAN, Environmental Science: Atmospheres, 3, 97-114, 10.1039/D2EA00063F, 2023.

Potosnak, M. J., LeStourgeon, L., Pallardy, S. G., Hosman, K. P., Gu, L., Karl, T., Geron, C., and Guenther, A. B.: Observed and modeled ecosystem isoprene fluxes from an oak-dominated temperate forest and the influence of drought stress, Atmos. Environ., 84, 314-322, https://doi.org/10.1016/j.atmosenv.2013.11.055, 2014.

Ramasamy, S., Ida, A., Jones, C., Kato, S., Tsurumaru, H., Kishimoto, I., Kawasaki, S., Sadanaga, Y., Nakashima, Y., Nakayama, T., Matsumi, Y., Mochida, M., Kagami, S., Deng, Y., Ogawa, S., Kawana, K., and Kajii, Y.:

Total OH reactivity measurement in a BVOC dominated temperate forest during a summer campaign, 2014, Atmos. Environ., 131, 41-54, https://doi.org/10.1016/j.atmosenv.2016.01.039, 2016.

Rinnan, R., Iversen, L. L., Tang, J., Vedel-Petersen, I., Schollert, M., and Schurgers, G.: Separating direct and indirect effects of rising temperatures on biogenic volatile emissions in the Arctic, Proc Natl Acad Sci U S A, 117, 32476-32483, 10.1073/pnas.2008901117, 2020.

Ruffault, J., Curt, T., Martin-StPaul, N. K., Moron, V., and Trigo, R. M.: Extreme wildfire events are linked to global-change-type droughts in the northern Mediterranean, Nat. Hazards Earth Syst. Sci., 18, 847-856, 10.5194/nhess-18-847-2018, 2018.

Safronov, A. N., Shtabkin, Y. A., Berezina, E. V., Skorokhod, A. I., Rakitin, V. S., Belikov, I. B., and Elansky, N. F.: Isoprene, Methyl Vinyl Ketone and Methacrolein from TROICA-12 Measurements and WRF-CHEM and GEOS-CHEM Simulations in the Far East Region, Atmosphere, 10, 152, 2019.

Sahu, A., Mostofa, M. G., Weraduwage, S. M., and Sharkey, T. D.: Hydroxymethylbutenyl diphosphate accumulation reveals MEP pathway regulation for high CO₂-induced suppression of isoprene emission, Proc. Natl. Acad. Sci., 120, e2309536120, doi:10.1073/pnas.2309536120, 2023.

Salvador, C. M., Chou, C. C. K., Ho, T. T., Tsai, C. Y., Tsao, T. M., and Su, T. C.: Contribution of Terpenes to Ozone Formation and Secondary Organic Aerosols in a Subtropical Forest Impacted by Urban Pollution, Atmosphere, 11, 1232, 2020a.

Salvador, C. M., Chou, C. C. K., Cheung, H. C., Ho, T. T., Tsai, C. Y., Tsao, T. M., Tsai, M. J., and Su, T. C.: Measurements of submicron organonitrate particles: Implications for the impacts of NOx pollution in a subtropical forest, Atmospheric Research, 245, 105080, https://doi.org/10.1016/j.atmosres.2020.105080, 2020b.

Salvador, C. M., Chou, C. C. K., Ho, T. T., Ku, I. T., Tsai, C. Y., Tsao, T. M., Tsai, M. J., and Su, T. C.: Extensive urban air pollution footprint evidenced by submicron organic aerosols molecular composition, npj Climate and Atmospheric Science, 5, 96, 10.1038/s41612-022-00314-x, 2022.

Sarris, D., Christopoulou, A., Angelonidi, E., Koutsias, N., Fulé, P. Z., and Arianoutsou, M.: Increasing extremes of heat and drought associated with recent severe wildfires in southern Greece, Regional Environmental Change, 14, 1257-1268, 10.1007/s10113-013-0568-6, 2014.

Selimovic, V., Yokelson, R. J., Warneke, C., Roberts, J. M., de Gouw, J., Reardon, J., and Griffith, D. W. T.: Aerosol optical properties and trace gas emissions by PAX and OP-FTIR for laboratory-simulated western US wildfires during FIREX, Atmos. Chem. Phys., 18, 2929-2948, 10.5194/acp-18-2929-2018, 2018.

Schneider, E., Czech, H., Popovicheva, O., Chichaeva, M., Kobelev, V., Kasimov, N., Minkina, T., Rüger, C. P., and Zimmermann, R.: Mass spectrometric analysis of unprecedented high levels of carbonaceous aerosol particles long-range transported from wildfires in the Siberian Arctic, Atmos. Chem. Phys., 24, 553-576, 10.5194/acp-24-553-2024, 2024a.

Schneider, S. R., Shi, B., and Abbatt, J. P. D.: The Measured Impact of Wildfires on Ozone in Western Canada from 2001 to 2019, J. Geophys. Res. Atmos., 129, e2023JD038866, https://doi.org/10.1029/2023JD038866, 2024b.

Seco, R., Karl, T., Guenther, A., Hosman, K. P., Pallardy, S. G., Gu, L., Geron, C., Harley, P., and Kim, S.: Ecosystem-scale volatile organic compound fluxes during an extreme drought in a broadleaf temperate forest of

the Missouri Ozarks (central USA), Global Change Biology, 21, 3657-3674, https://doi.org/10.1111/gcb.12980, 2015.

Selimovic, V., Ketcherside, D., Chaliyakunnel, S., Wielgasz, C., Permar, W., Angot, H., Millet, D. B., Fried, A., Helmig, D., and Hu, L.: Atmospheric biogenic volatile organic compounds in the Alaskan Arctic tundra: constraints from measurements at Toolik Field Station, Atmos. Chem. Phys., 22, 14037-14058, 10.5194/acp-22-14037-2022, 2022.

Sharkey, T. D., Wiberley, A. E., and Donohue, A. R.: Isoprene Emission from Plants: Why and How, Annals of Botany, 101, 5-18, 10.1093/aob/mcm240, 2007.

Shen, L., Mickley, L. J., and Murray, L. T.: Influence of 2000–2050 climate change on particulate matter in the United States: results from a new statistical model, Atmos. Chem. Phys., 17, 4355-4367, 10.5194/acp-17-4355-2017, 2017.

Shtabkin, Y. A., Safronov, A. N., Berezina, E. V., and Skorokhod, A. I.: The comparison between the isoprene, methyl vinyl ketone and methacrolein concentrations measured in the TROICA-12 expedition at Far East region, IOP Conference Series: Earth and Environmental Science, 231, 012047, 10.1088/1755-1315/231/1/012047, 2019.

Sinha, V., Williams, J., Lelieveld, J., Ruuskanen, T. M., Kajos, M. K., Patokoski, J., Hellen, H., Hakola, H., Mogensen, D., Boy, M., Rinne, J., and Kulmala, M.: OH Reactivity Measurements within a Boreal Forest: Evidence for Unknown Reactive Emissions, Environ. Sci. Technol., 44, 6614-6620, 10.1021/es101780b, 2010.

Spirig, C., Guenther, A., Greenberg, J. P., Calanca, P., and Tarvainen, V.: Tethered balloon measurements of biogenic volatile organic compounds at a Boreal forest site, Atmos. Chem. Phys., 4, 215-229, 10.5194/acp-4-215-2004, 2004.

Stein, A., Draxler, R. R., Rolph, G. D., Stunder, B. J., Cohen, M., and Ngan, F.: NOAA's HYSPLIT atmospheric transport and dispersion modeling system, Bulletin of the American Meteorological Society, 96, 2059-2077, 2015.

Stockwell, C. E., Veres, P. R., Williams, J., and Yokelson, R. J.: Characterization of biomass burning emissions from cooking fires, peat, crop residue, and other fuels with high-resolution proton-transfer-reaction time-of-flight mass spectrometry, Atmospheric Chemistry and Physics, 15, 845-865, 10.5194/acp-15-845-2015, 2015.

Taipale, R., Ruuskanen, T. M., Rinne, J., Kajos, M. K., Hakola, H., Pohja, T., and Kulmala, M.: Technical Note: Quantitative long-term measurements of VOC concentrations by PTR-MS – measurement, calibration, and volume mixing ratio calculation methods, Atmos. Chem. Phys., 8, 6681-6698, 10.5194/acp-8-6681-2008, 2008.

Takeuchi, M., Berkemeier, T., Eris, G., and Ng, N. L.: Non-linear effects of secondary organic aerosol formation and properties in multi-precursor systems, Nature Communications, 13, 7883, 10.1038/s41467-022-35546-1, 2022.

Varga, K., Jones, C., Trugman, A., Carvalho, L. M. V., McLoughlin, N., Seto, D., Thompson, C., and Daum, K.: Megafires in a Warming World: What Wildfire Risk Factors Led to California's Largest Recorded Wildfire, Fire, 5, 16, 2022.

Vermeuel, M. P., Novak, G. A., Kilgour, D. B., Claflin, M. S., Lerner, B. M., Trowbridge, A. M., Thom, J., Cleary, P. A., Desai, A. R., and Bertram, T. H.: Observations of biogenic volatile organic compounds over a mixed temperate forest during the summer to autumn transition, Atmos. Chem. Phys., 23, 4123-4148, 10.5194/acp-23-4123-2023, 2023.

Voliotis, A., Wang, Y., Shao, Y., Du, M., Bannan, T. J., Percival, C. J., Pandis, S. N., Alfarra, M. R., and McFiggans, G.: Exploring the composition and volatility of secondary organic aerosols in mixed anthropogenic and biogenic precursor systems, Atmos. Chem. Phys., 21, 14251-14273, 10.5194/acp-21-14251-2021, 2021.

Wang, H., Ma, X., Tan, Z., Wang, H., Chen, X., Chen, S., Gao, Y., Liu, Y., Liu, Y., Yang, X., Yuan, B., Zeng, L., Huang, C., Lu, K., and Zhang, Y.: Anthropogenic monoterpenes aggravating ozone pollution, National Science Review, 9, 10.1093/nsr/nwac103, 2022.

Wang, N., Zannoni, N., Ernle, L., Bekö, G., Wargocki, P., Li, M., Weschler, C. J., and Williams, J.: Total OH Reactivity of Emissions from Humans: In Situ Measurement and Budget Analysis, Environ. Sci. Technol., 55, 149-159, 10.1021/acs.est.0c04206, 2021.

Wang, Z., Wang, Z., Zou, Z., Chen, X., Wu, H., Wang, W., Su, H., Li, F., Xu, W., Liu, Z., and Zhu, J.: Severe Global Environmental Issues Caused by Canada's Record-Breaking Wildfires in 2023, Advances in Atmospheric Sciences, 10.1007/s00376-023-3241-0, 2023.

Wells, K. C., Millet, D. B., Cady-Pereira, K. E., Shephard, M. W., Henze, D. K., Bousserez, N., Apel, E. C., de Gouw, J., Warneke, C., and Singh, H. B.: Quantifying global terrestrial methanol emissions using observations from the TES satellite sensor, Atmos. Chem. Phys., 14, 2555-2570, 10.5194/acp-14-2555-2014, 2014.

Wennberg, P. O., Bates, K. H., Crounse, J. D., Dodson, L. G., McVay, R. C., Mertens, L. A., Nguyen, T. B., Praske, E., Schwantes, R. H., and Smarte, M. D.: Gas-phase reactions of isoprene and its major oxidation products, Chem. Rev., 118, 3337-3390, 2018.

Wiedinmyer, C., Tie, X., Guenther, A., Neilson, R., and Granier, C.: Future Changes in Biogenic Isoprene Emissions: How Might They Affect Regional and Global Atmospheric Chemistry?, Earth Interactions, 10, 1-19, https://doi.org/10.1175/EI174.1, 2006.

Wiedinmyer, C., Greenberg, J., Guenther, A., Hopkins, B., Baker, K., Geron, C., Palmer, P. I., Long, B. P., Turner, J. R., Pétron, G., Harley, P., Pierce, T. E., Lamb, B., Westberg, H., Baugh, W., Koerber, M., and Janssen, M.: Ozarks Isoprene Experiment (OZIE): Measurements and modeling of the "isoprene volcano", J. Geophys. Res. Atmos., 110, https://doi.org/10.1029/2005JD005800, 2005.

Worton, D. R., Moreno, S., O'Daly, K., and Holzinger, R.: Development of an International System of Units (SI)-traceable transmission curve reference material to improve the quantitation and comparability of proton-transfer-reaction mass-spectrometry measurements, Atmos. Meas. Tech., 16, 1061-1072, 10.5194/amt-16-1061-2023, 2023.

Yang, G., Huo, J., Wang, L., Wang, Y., Wu, S., Yao, L., Fu, Q., and Wang, L.: Total OH Reactivity Measurements in a Suburban Site of Shanghai, J. Geophys. Res. Atmos., 127, e2021JD035981, https://doi.org/10.1029/2021JD035981, 2022.

962 Yokelson, R. J., Christian, T. J., Karl, T. G., and Guenther, A.: The tropical forest and fire emissions experiment:
963 laboratory fire measurements and synthesis of campaign data, Atmos. Chem. Phys., 8, 3509-3527, 10.5194/acp-
964 8-3509-2008, 2008.
965 Yu, H., Ortega, J., Smith, J. N., Guenther, A. B., Kanawade, V. P., You, Y., Liu, Y., Hosman, K., Karl, T., Seco, R.,
966 Geron, C., Pallardy, S. G., Gu, L., Mikkilä, J., and Lee, S.-H.: New Particle Formation and Growth in an
967 Isoprene-Dominated Ozark Forest: From Sub-5 nm to CCN-Active Sizes, Aerosol Science and Technology, 48,
968 1285-1298, 10.1080/02786826.2014.984801, 2014.
969 Yuan, B., Koss, A. R., Warneke, C., Coggon, M., Sekimoto, K., and de Gouw, J. A.: Proton-Transfer-Reaction Mass
970 Spectrometry: Applications in Atmospheric Sciences, Chem. Rev., 117, 13187-13229,
971 10.1021/acs.chemrev.7b00325, 2017.
972